N93-18937

CSI/MMC Studies for Improving Jitter Performance for Large Multi-Payload Platforms

FINAL REPORT

JOHN CHIONCHIO
MICHAEL GARNEK

MIRROR MOTION COMPENSATION

AGENDA

- INTRODUCTION TO MIRROR MOTION COMPENSATION
- EOS PLATFORM MODEL AND DISTURBANCE DEFINITION
- INSTRUMENT JITTER RESPONSE
- MODELING UNCERTAINTIES
  - FREQUENCY
  - DAMPING
  - LAG FILTER
  - MIRROR INERTIA
- MULTIPLE DISTURBANCES
- FEEDBACK
- SUMMARY

ACKNOWLEDGEMENTS

This study was performed under NASA contract number NAS5-32500, task assignment 003, Development of Dynamic Spacecraft Models, under the direction of William Grantham, Deputy Head CSIO, NASA Langley Research Center.

Original members of the GE Astro Space team who made significant contributions to the study are Dennis Hill and David Breskman.

PRECEDING PAGE BLANK NOT FILMED

INTRODUCTION

The objective of the study was to demonstrate the feasibility of the Mirror Motion Compensation (MMC) technique for the reduction or suppression of instrument on-orbit jitter. Future remote sensing spacecraft consisting of large platforms with multiple payloads will be required to meet tight jitter constraints, typically less than 0.1 arc seconds. Mirror Motion Compensation provides a method which may prove useful in meeting these future requirements. The MMC technique features a central compensation logic which predicts instrument response to known disturbances and modifies the line of sight of the affected instruments accordingly to compensate for the disturbance.

MIRROR MOTION COMPENSATION

- **OBJECTIVES**

  1. **DEMONSTRATE FEASIBILITY OF MMC TECHNIQUE TO REDUCE ON - ORBIT INSTRUMENT JITTER**
  2. **INVESTIGATE THE USE OF SPACECRAFT FLEXIBLE MODES**
  3. **INVESTIGATE THE SENSITIVITY OF MMC TECHNIQUE TO MODELING ERRORS**

INTRODUCTION

Instrument jitter, or the rotational response of an instrument to a disturbance, must be controlled if maximum instrument performance is to be expected. Control and suppression of jitter effects have become increasingly important for the following reasons:

1. Increased pointing accuracy requirements on instruments.
2. Multiple disturbance sources, in the form of slewing sensors and internal instrument disturbances (cryo-coolers), present on the same platform.
3. Trends toward large, flexible orbiting platforms subject to significant response from both rigid body motion and flexible modes of vibration.

The approach used in the study featured the application of the MMC technique to instruments on-board the EOS A-1 platform. The EOS A-1 spacecraft was an appropriate choice since it represents the class of large flexible space platforms mounting multiple instruments with stringent pointing requirements subject to multiple vibration disturbance sources.

- **WHY USE MMC?**

  SUPPRESSION OF JITTER HAS BECOME INCREASINGLY IMPORTANT FOR THE FOLLOWING REASONS:

  1. **INSTRUMENTS WITH MORE STRINGENT POINTING REQUIREMENTS.**
  2. **TRENDS TOWARD LARGER PLATFORMS WITH MULTIPLE DISTURBANCE SOURCES.**
  3. **TRENDS TOWARD SPACECRAFT WITH LARGE FLEXIBLE APPENDAGES.**

- **APPROACH**

  EOS A-1 DYNAMIC MODEL WITH INTEGRAL ACS CONTROLLER USED AS A GENERIC LARGE SPACE STRUCTURE.

SPACECRAFT FEEDBACK CONTROL VERSUS OPEN LOOP MMC

The MMC technique features a centralized compensation logic which simulates the response of the platform to a disturbance (or multiple disturbances) in real time and modifies the lines of sight of the affected instruments. The disturbance torques, platform dynamics, and sensor dynamics must be known. This knowledge is used by the compensation logic program to predict the response of a given sensor to a disturbance. The compensation logic uses the response predictions to issue sensor motion commands which counteract the disturbance response and suppress instrument jitter. Note that there is no feedback from the controlled instrument to the compensation logic program. This is a salient feature of the MMC system which distinguishes it from more traditional control approaches. The advantage is that if no feedback is employed then the feedback sensors are unnecessary, thus saving cost, weight, and providing a simpler control system.

Clearly, the MMC system is best applied in cases where the disturbances are deterministic and the spacecraft dynamic characteristics are well known and accurately modeled.

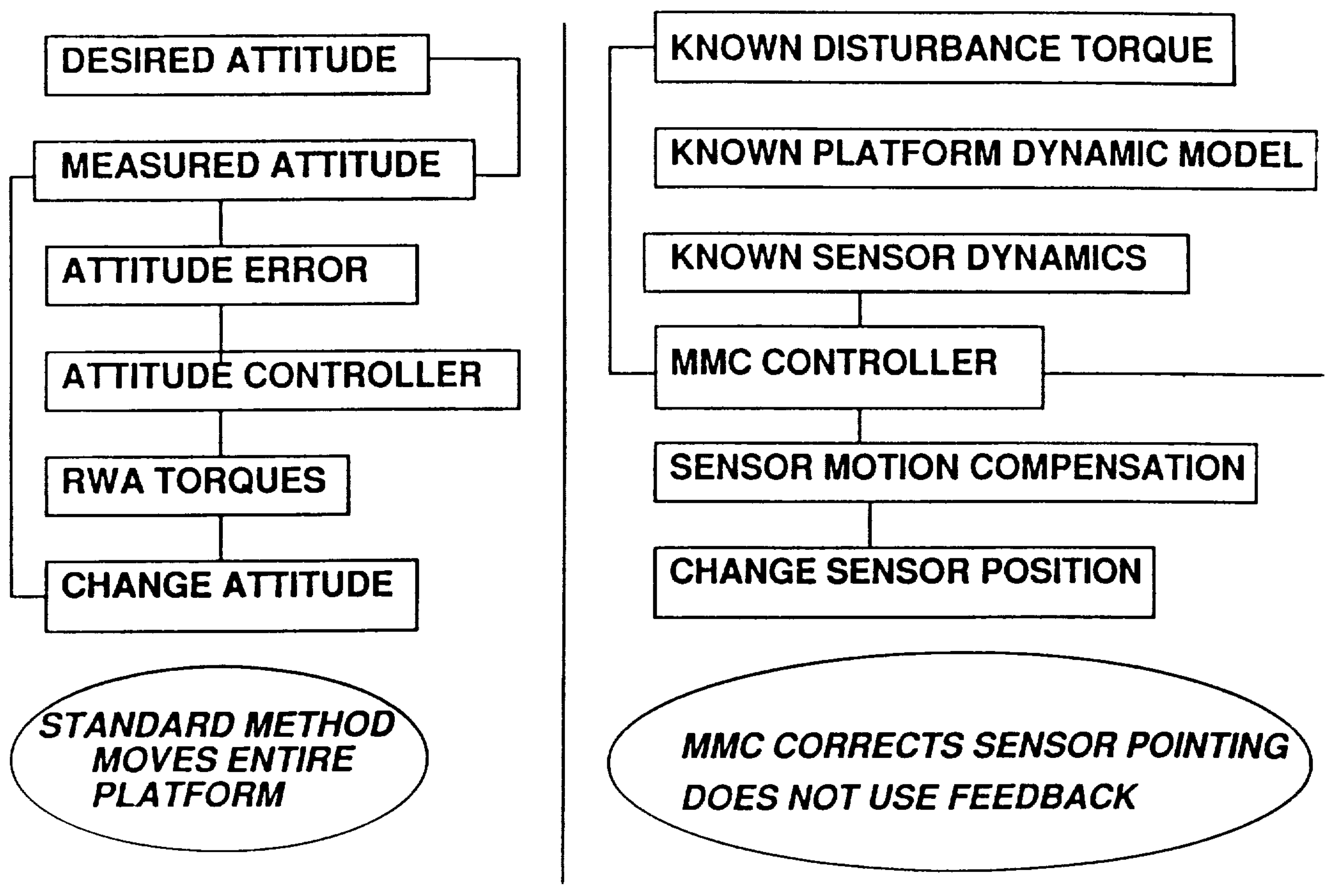

AMSU DISTURBANCE

Of significantly higher frequency, the AMSU disturbance is also a roll axis torque disturbance. The significant action for this disturbance occurs over approximately 8 seconds, as contrasted with the MODIS-T, which requires almost 400 seconds to complete its cycle. The disturbance profile is analytically determined and provided by the instrumenter.

The AMSU instrument module contains three mirrors which rotate continuously in one direction about a line parallel to the spacecraft roll axis. The AMSU A-1 has 2 of the scan mirrors and its scan profile, shown on the facing page, represents the disturbance due to both mirrors combined. All mirrors have a scan cycle (360 degree rotation) period of 8 seconds during which time their angular speed varies. For all mirrors, a scan cycle starts with an Earth scan whereby they are stepped 30 times to cover 99.9 degrees with NADIR in the middle. This is followed by cold and hot calibrations at constant angular speed in between which are accelerations and decelerations. These calibration torques move the mirrors the remaining 260.1 degrees, returning them to their original position. This entire scan pattern is repeated every 8 seconds.

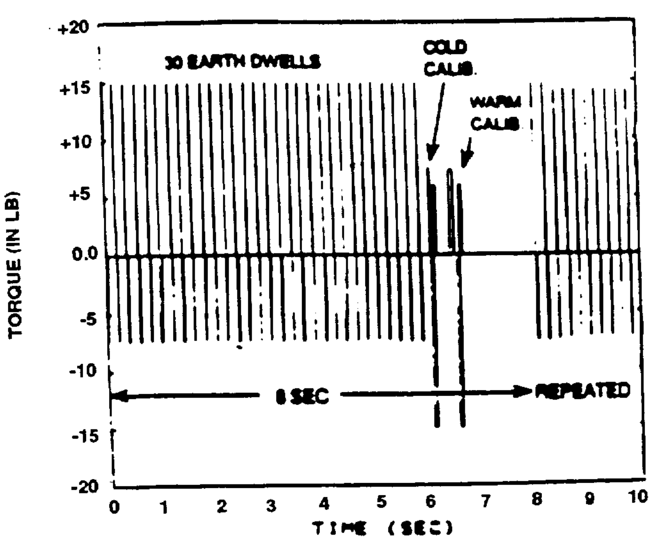

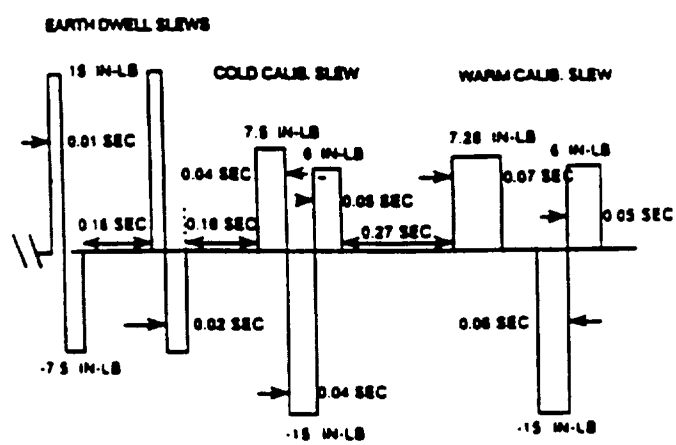

EOS SPACECRAFT

The illustration depicts the EOS A-1 spacecraft and the reference coordinate axes defining the roll, pitch, and yaw degrees of freedom. The EOS A-1 is a large platform, 38 feet long, 10 feet in diameter, and weighing 33,000 lbs. Originally designed for launch on the Titan booster, the design features a truss structure with graphite-epoxy tubes connected via titanium cluster fittings at the truss joints. Precision mounting platforms consisting of plates of lightweight aluminum honeycomb core with graphite-epoxy skins span the truss and provide surfaces for instrument mounting as shown. Of particular interest in this study are the AMSU, MODIS-T, and CERES instruments. The study focuses on the roll and yaw axis jitter of the CERES subject to vibration disturbance from both the AMSU and MODIS-T.

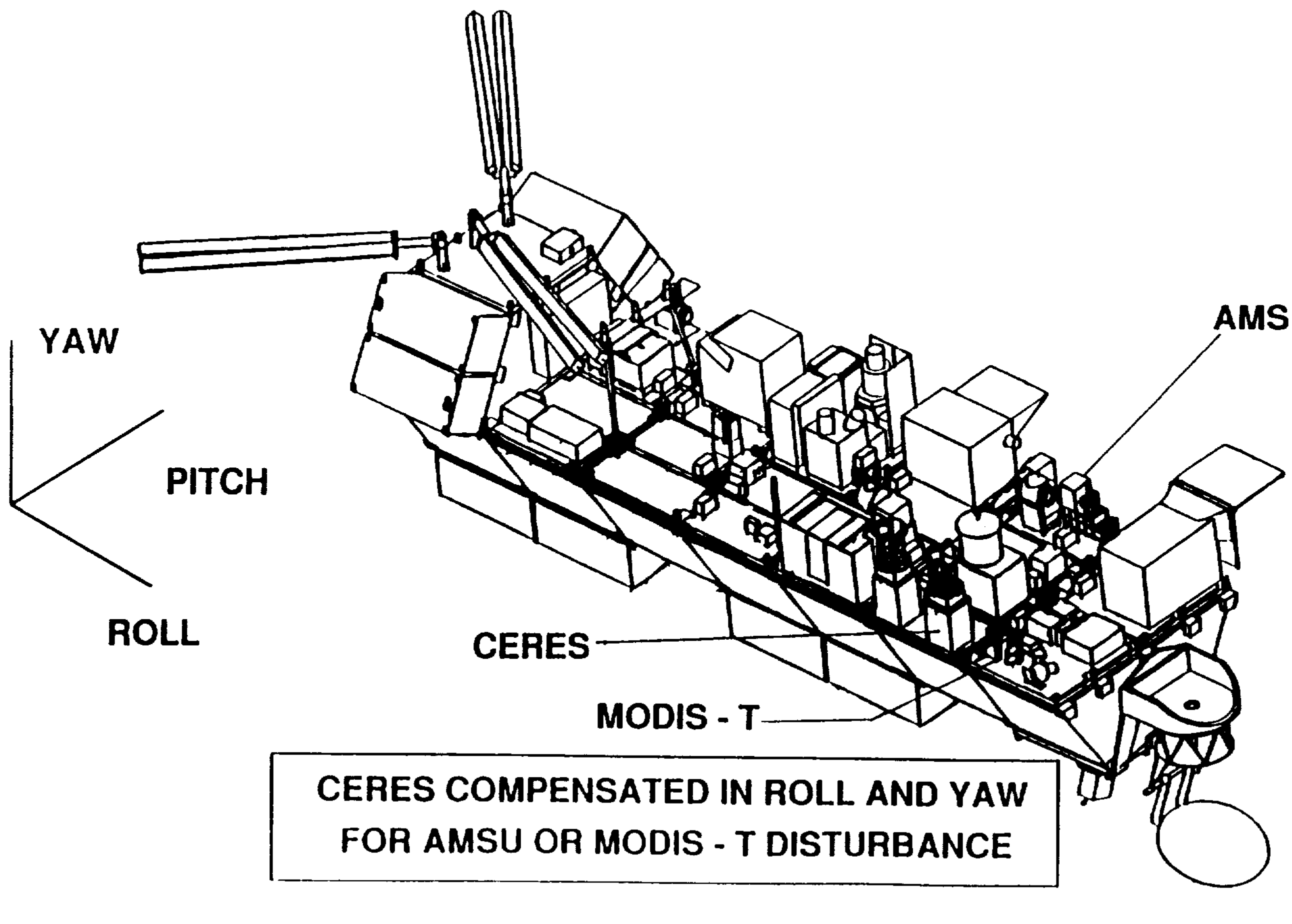

CERES COMPENSATED IN ROLL AND YAW
FOR AMSU OR MODIS - T DISTURBANCE

DISTURBANCE AND RESPONSE

Criteria were established for both the subject instrument and the disturbance sources in this study. Disturbance criteria focused on spacecraft components which produce significant vibration which is then transmitted to other instruments through the spacecraft structure. In addition to being major sources of jitter, the disturbance sources should represent a broad spectrum of vibration frequency components. MODIS-T and AMSU were found in combination to fulfill these requirements. Both are scanning instruments which produce significant vibration. The MODIS-T vibration provides the low frequency components and AMSU is responsible for the higher frequencies.

The CERES was chosen as the subject instrument for jitter compensation since it completely satisfied the criteria, which required an instrument which suffered from significant jitter and had a 2 axis gimbal at which the compensation could be applied to suppress the jitter. The CERES degrees of freedom corresponding to the 2 axis gimbal are about the spacecraft roll and yaw axes previously depicted.

DISTURBANCE CRITERIA

- CHOOSE COMPONENTS WHICH ARE MAJOR DISTURBERS
- CAPTURE BOTH HIGH AND LOW FREQUENCY INPUTS

RESPONSE CRITERIA

- CHOOSE INSTRUMENT WITH SIGNIFICANT JITTER
- CHOOSE INSTRUMENT WITH 2 AXIS GIMBAL

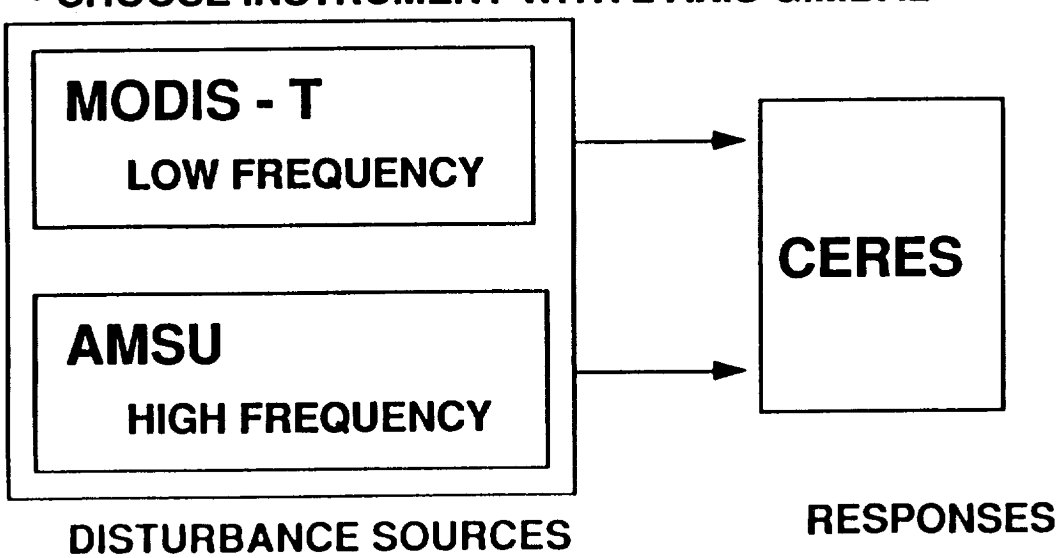

EOS A-1 FINITE ELEMENT MODEL

A large and detailed structural finite element model of the EOS A-1 was available from previous EOS jitter studies. The model contains 11900 nodes and 14400 elements, and simulates the spacecraft in the on orbit configuration with the solar array deployed and oriented as shown. Normal modes analysis yields 655 modes up to a frequency of 150 Hertz.

A dynamic modal model consisting of 172 modal degrees of freedom and 655 mass normalized modes was obtained from the structural finite element model. The 172 modal degrees of freedom constitute the points of interest, such as instrument locations, reaction wheel locations, and spacecraft center of gravity, relevant to the problem. This dynamic model was designated EOS 5.

The modal model describes the dynamic relationships between the disturbance sources and the affected instruments, spacecraft structure, and control sensors and actuators via the chosen degrees of freedom and the associated normal mode shapes. Solar array modes were retained up to 3 Hertz and spacecraft primary structure modes were retained up to 150 Hertz in order to obtain acceptable dynamic fidelity up to 120 Hertz, the highest significant component of the Stirling-cycle cyro-cooler.

The 655 mass normalized modes include 6 rigid body modes of the unconstrained spacecraft structure as well as 11 so called gimbal modes (only 2 were used in this study). The gimbal modes represent the displacement of the instrument scanning element degree of freedom relative to the spacecraft. Since the scanning elements must be free to rotate relative to the spacecraft in order to compensate for the spacecraft rotation, these degrees of freedom yield a zero frequency mode for each free axis of rotation. Certain instruments, such as CERES, have 2 axis gimbals and thus produce 2 gimbal modes. Other instruments rotate about a single axis and contribute only one mode to the gimbal mode set.

- FEM COMPOSED OF 11900 NODES AND 14400 ELEMENTS
- NORMAL MODES ANALYSIS YIELDS 655 MODES UP TO 150 HERTZ

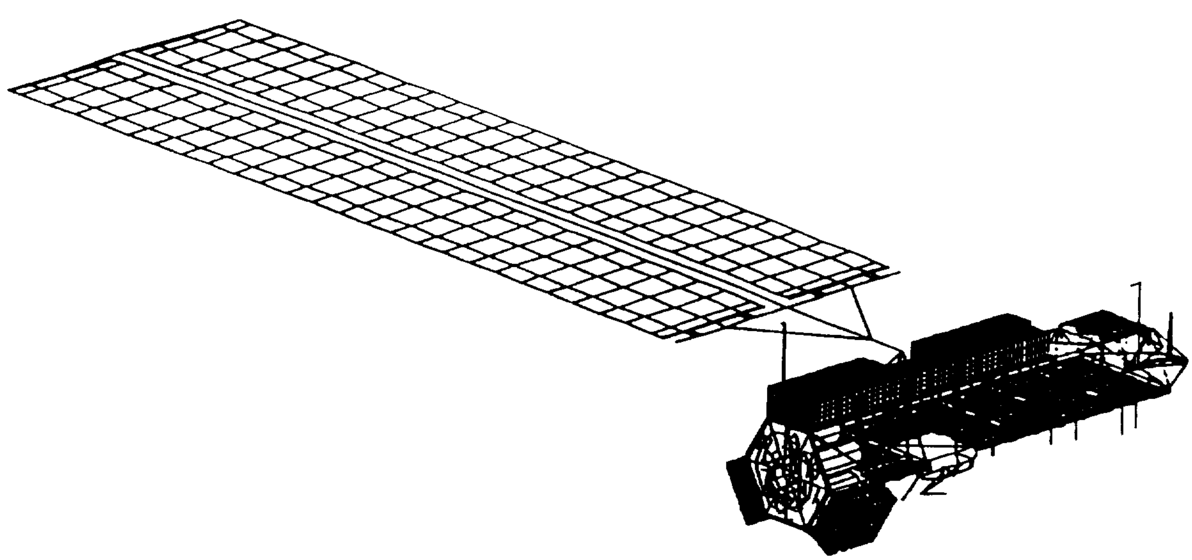

LARGE FEM NEEDED TO OBTAIN HIGH FREQUENCY MODES FOR EOS STIRLING COOLER STUDY

FUNDAMENTAL SOLAR ARRAY MODE

The remaining 638 modes are flexible structural modes divided between the solar array (109 modes) and the primary structure (529 modes). Of these modes a subset was found, by a modal significance survey, to be important for the jitter predictions. The fundamental solar array mode, shown in the illustration, occurred at a frequency of .208 Hertz. As can be clearly seen in the mode shape plot, this mode would naturally contribute significantly to instrument roll axis jitter. This mode was in fact the only significant mode for the lower frequency MODIS-T disturbance, and accurate predictions of jitter were possible using only this mode and the 17 rigid body and gimbal modes in the dynamic simulation. The AMSU disturbance, however, required that 5 flexible modes be retained to ensure dynamic fidelity. The AMSU mode set included the fundamental solar array mode, as well as several higher flexible modes, reflecting the higher frequency content of this disturbance.

The complete dynamic model includes the modal model generated from the FEM and the algorithms to control the attitude of the EOS-A1. The ACS controller features a proportional double integral derivative controller with a 4th order structural filter and results in a closed loop bandwidth of 0.03 Hertz, originally chosen to be about one tenth of the fundamental solar array frequency. The ACS controller is implemented in a state-space formulation, and accepts outputs from gyroscopic sensors and generates torque commands to reaction wheels.

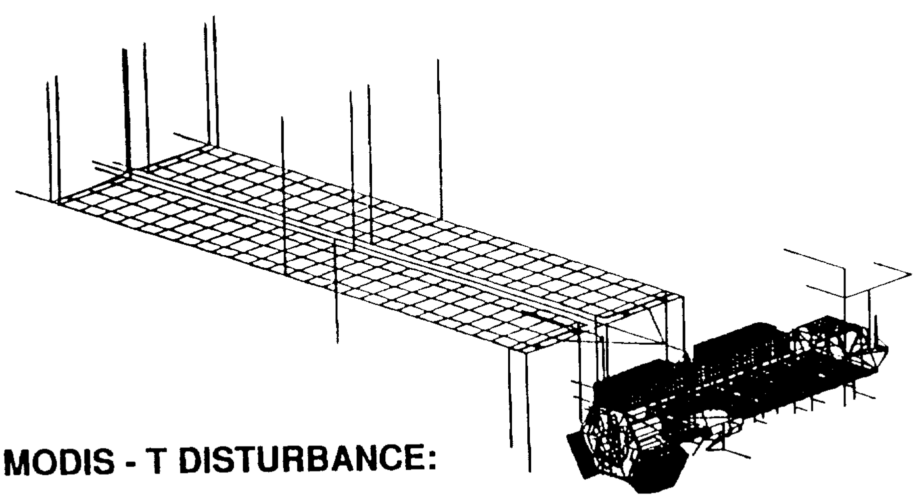

FOR MODIS - T DISTURBANCE:

FUNDAMENTAL SOLAR ARRAY MODE AT 0.208 HERTZ DOMINANT FOR ROLL RESPONSE

FOR AMSU DISTURBANCE:

MODES 22 (0.208 HZ), 42 (1.0 HZ), 150 (31.6 HZ), 153 (33.6 HZ) AND 155 (36.1 HZ) DOMINANT FOR ROLL RESPONSE

MODIS-T DISTURBANCE

As previously stated, the MMC technique is best suited to cases where the disturbances are deterministic. In this case, the MODIS-T disturbance is well known and regular. The result of a scanning mirror slew, the disturbance inputs roll axis torque disturbances as shown. The disturbance profile is analytically determined and provided by the instrumenter.

The diffuser mechanism within the MODIS-T instrument rotates back and forth about a line parallel to the spacecraft roll axis. The instrument takes data for about 40 % of a full orbit and only on the day side of the orbit. There is a calibration deployment over the equator lasting 3 minutes.

The disturbance torque, which is shown on the facing page, moves the MODIS-T diffuser mechanism 180 degrees in 90 seconds to its deployed position and remains in this position for 3 minutes over the equator for solar calibration. The disturbance torque is then applied again with the sign reversed to return the MODIS-T to its original position. This procedure may occur as often as once per orbit, or only once per solar day.

MODIS - T DIFFUSER MECHANISM TORQUE PROFILE

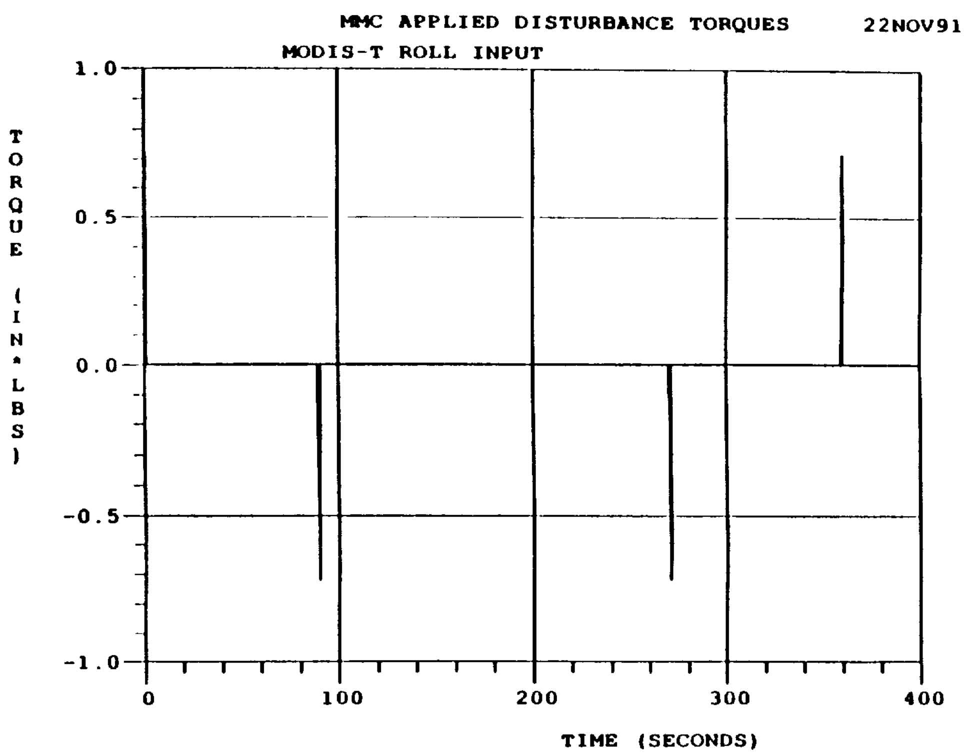

UNCOMPENSATED CERES RESPONSE TO MODIS-T INPUT

The dynamic model specified by the mode shapes and associated frequencies was input to the dynamic software simulator. The simulator is based on standard GE software packages of FORTRAN subroutines for the manipulation of large matrices and the solution of the equations of motion for a many degree of freedom system. The solution technique relies on an exact inverse Laplace transform method and is performed in the modal space on mass normalized modes, thereby taking advantage of the decoupling afforded by this technique. The disturbance is converted into a modal admittance and applied to the equations, the solution of which yields the modal acceleration, velocity, and position as a function of time. The modal coordinates are transformed to the appropriate physical coordinates and plotted as shown on the facing figure.

The time history plot predicts the response of the dynamic model degree of freedom representing the CERES roll displacement subject to the MODIS-T disturbance. This is the baseline response representing the jitter which would occur without any compensation applied. It can be observed that the response consists of a rigid body displacement with flexible modes superposed. In fact, detailed analysis reveals that the fundamental solar array mode is responsible for almost all of the flexible component of the response. The spacecraft navigation and guidance controller effect is evident as the rigid body portion of the response is seen to decay and by approximately 600 seconds only the flexible response remains.

UNCOMPENSATED CERES RESPONSE TO MODIS - T DISTURBANCE

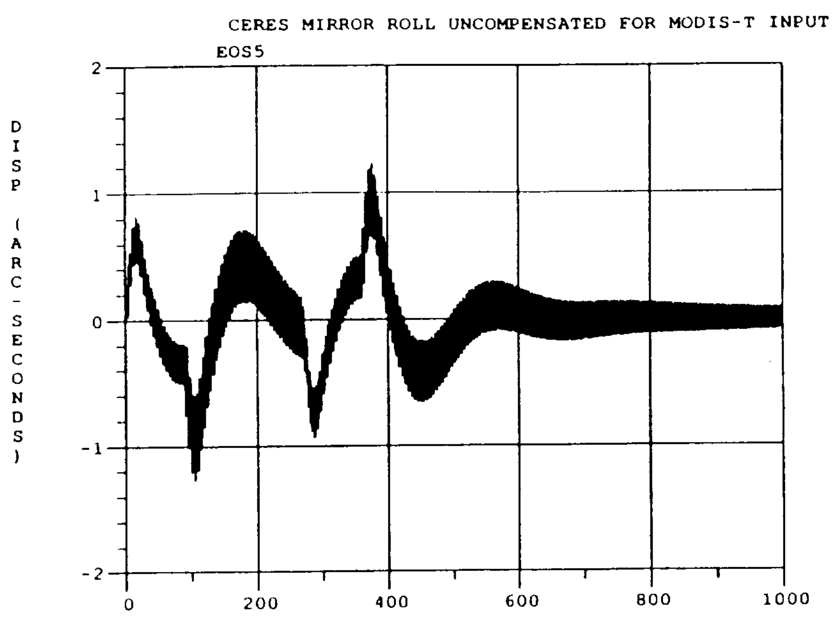

MODIS - T DISTURBANCE EXCITES LOW FREQUENCY SOLAR ARRAY MODE

MODIS-T AND AMSU COMPARED

To further illustrate the contrast between the two disturbances, both profiles were plotted on the same time and magnitude axes. One "spike" of the MODIS-T disturbance is represented by the dotted line, which can be seen overlapping 5 "spikes" of the significantly larger AMSU disturbance. The high frequency nature of the AMSU disturbance is readily apparent.

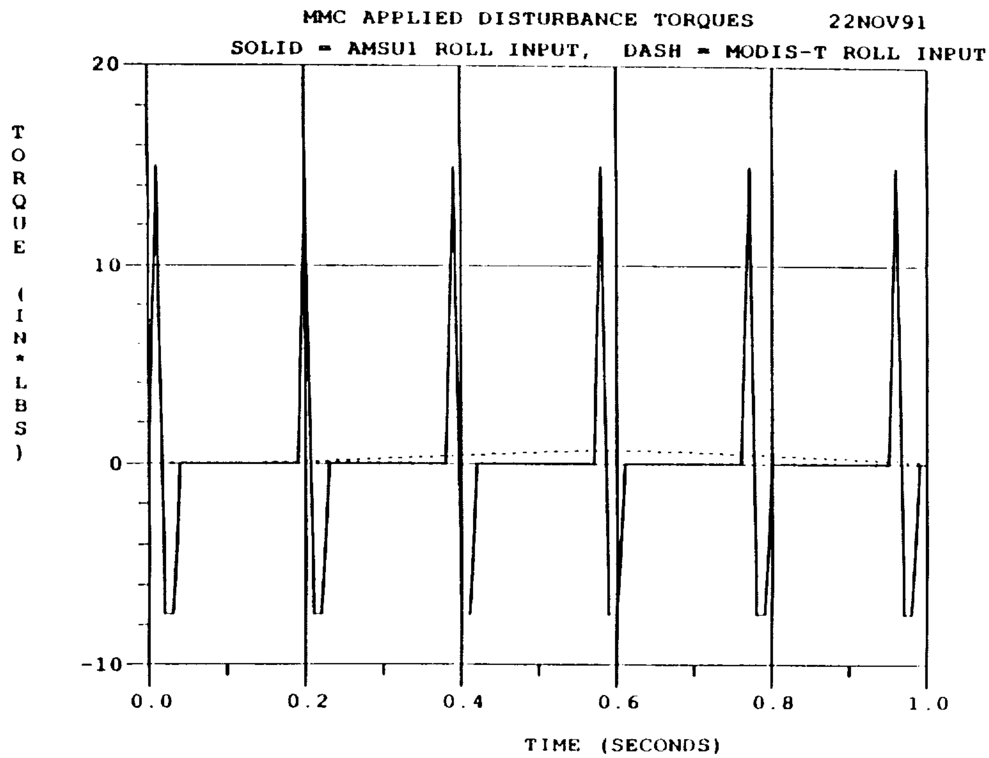

C-3

COMPENSATED CERES RESPONSE TO MODIS-T DISTURBANCE
RIGID BODY MODES ONLY

The application of mirror motion compensation proceeds differently from the simple uncompensated run. First a "predictor" dynamic model is solved for the time history of the degree of freedom in question (in this case, the CERES response to the MODIS-T disturbance). This predictor model is not necessarily the full 655 mode dynamic model of the baseline run, but can be a subset of it. The predictor model simulates the MMC centralized compensation logic. The solution of the predictor model provides the rotational acceleration of the degrees of freedom in question. These accelerations are combined with the known sensor dynamics to calculate a torque function of time. The torque function is stored and the full 655 modes "truth" model is then run through the simulator. The torques from the predictor model are applied to the appropriate sensor gimbal degrees of freedom in the truth model, but in the opposite sense. The gimbal degrees of freedom are free to rotate under the action of the torques in this model (unlike the predictor model where they are locked), thus the ensuing motion of the sensor compensates for the motion of the spacecraft caused by the disturbance. The modal displacements of the truth model are calculated and converted to physical displacements and plotted as shown.

In this case, the predictor model consisted of only the spacecraft and gimbal rigid body modes. The compensating torques derived from the predictor model thus can only, at best, null out the rigid body portion of the disturbance. This is in fact what occurs as demonstrated in the plot of the CERES roll response to MODIS-T disturbance as predicted by the truth model. Note that the rigid body component is effectively eliminated when compared with the baseline response. The flexible component decays slowly, due to the light damping of 0.15% critical. The damping is applied as modal damping, with all modes having the same damping value.

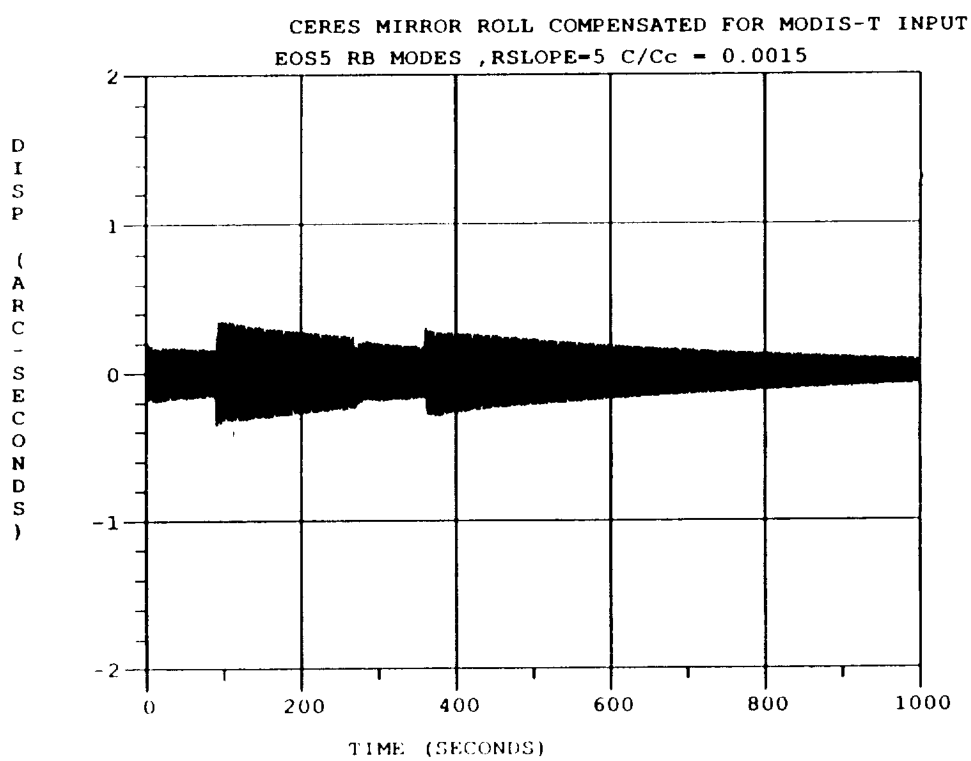

RIGID BODY MODES EFFECTIVELY COMPENSATED

COMPENSATED CERES RESPONSE TO MODIS-T DISTURBANCE
RIGID BODY PLUS FLEXIBLE MODE 22(.208HZ)

The sophistication of the predictor model was increased by adding the fundamental solar array mode. The motion predicted now includes information about the flexible component of the response and the compensating torques are dramatically effective at reducing jitter when applied in the truth model. This dramatic decrease in response is due to perfect knowledge of the platform and sensor dynamics. The reason for the small residual error is due to the effects of gimbal motor rise time and the secondary torque effects on the platform, which are discussed in more detail in the next chart.

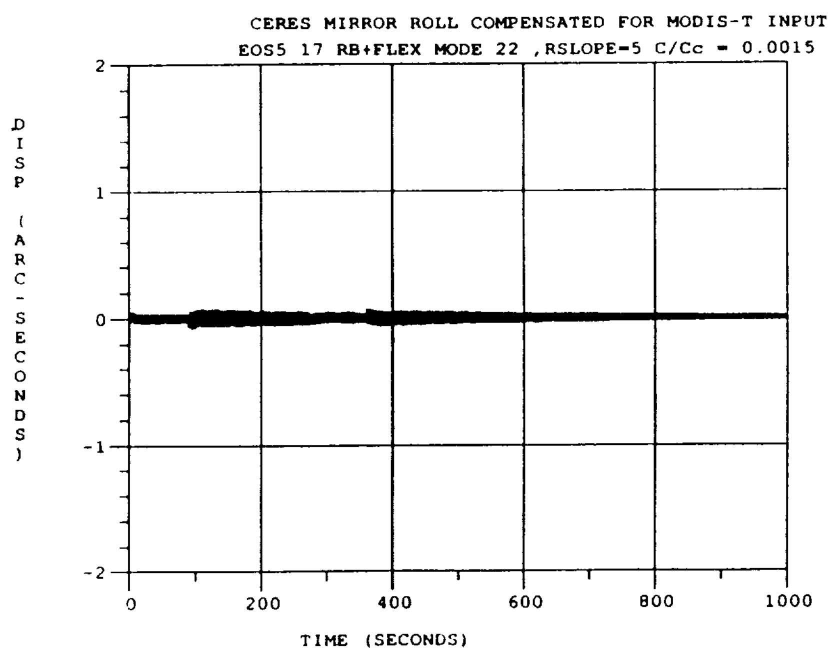

LARGE REDUCTION IN JITTER WITH ONE FLEXIBLE MODE COMPENSATED

COMPENSATED CERES RESPONSE TO MODIS-T DISTURBANCE
RIGID BODY PLUS ALL FLEXIBLE MODES

The predictor model now uses all of the modes and is identical to the truth model. Only slight jitter reduction improvement is obtained. We can conclude that the fundamental solar array mode is the dominant mode with regard to the CERES - MODIS-T disturbance relation. Jitter is still present despite the fact that the predictor and truth models are identical. The jitter results from two sources. The compensation motion of the mirrors affects the spacecraft as another disturbance source of both rigid body and flexible motion. This source is not accounted for in the predictor model. A second source of errors occurs due to the finite rise time of the motors that move the mirrors. Since the torques in reality cannot be applied instantaneously, a lag filter is used in the simulation to model these effects. The torque commands must pass through this lag filter before they are applied to the gimbal degrees of freedom in the truth model. The lag filter has a time constant, represented by the RSLOPE value, and attenuates the torque to simulate actual motor behavior. The time constant is set at 200 milliseconds baseline, corresponding to an RSLOPE value of 5 as noted on the plot. The predictor model does not account for the lag filter.

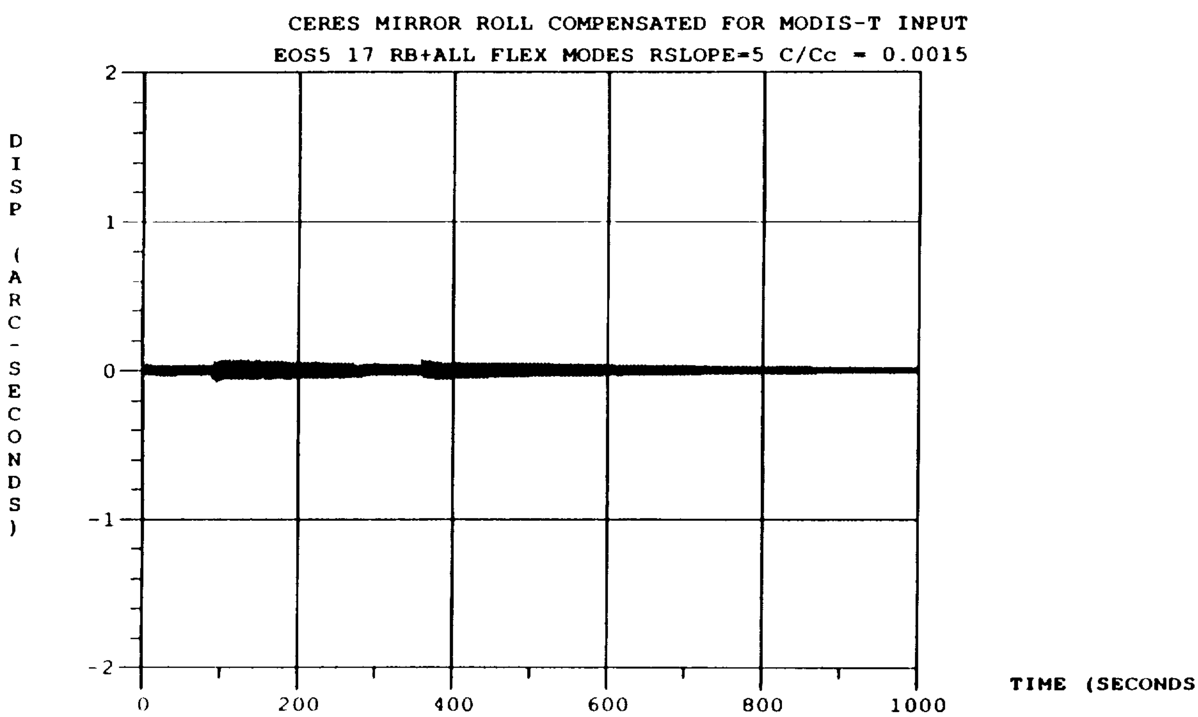

MARGINAL IMPROVEMENT WITH ALL FLEXIBLE MODES
MODE 22 DOMINANT

SUMMARY TABLE OF CERES RESPONSE TO MODIS-T DISTURBANCE

Tabular data is provided to more readily ascertain the effectiveness of the MMC scheme. For a moving sample window 1 second wide the jitter was reduced by a factor greater than 5 for a predictor model with all rigid body and the fundamental solar array modes. Longer duration windows describe the stability of the system, and an improvement can be seen for stability by a factor of 17.

MODEL	JITTER IN ARC SECONDS WINDOW SIZE (SECONDS)			
	1.0	9.0	60.0	1000.0
UNCOMPENSATED	0.4698	1.0047	1.9449	2.4977
RIGID BODY MODES	0.4159	0.6960	0.6984	0.6984
RB + MODE 22	0.0866	0.1438	0.1492	0.1492
RB + ALL MODES	0.0842	0.1421	0.1458	0.1458

MMC TECHNIQUE REDUCES JITTER AND IMPROVES STABILITY

UNCOMPENSATED CERES RESPONSE TO AMSU DISTURBANCE

Baseline plot of the CERES roll response to the AMSU disturbance as predicted by the truth model again shows the effect of superimposed flexible and rigid body modes. The response shows the fundamental solar array mode at 0.208 Hz as well as higher frequency modes. The response is significantly smaller than that due to the MODIS-T disturbance, but higher in frequency.

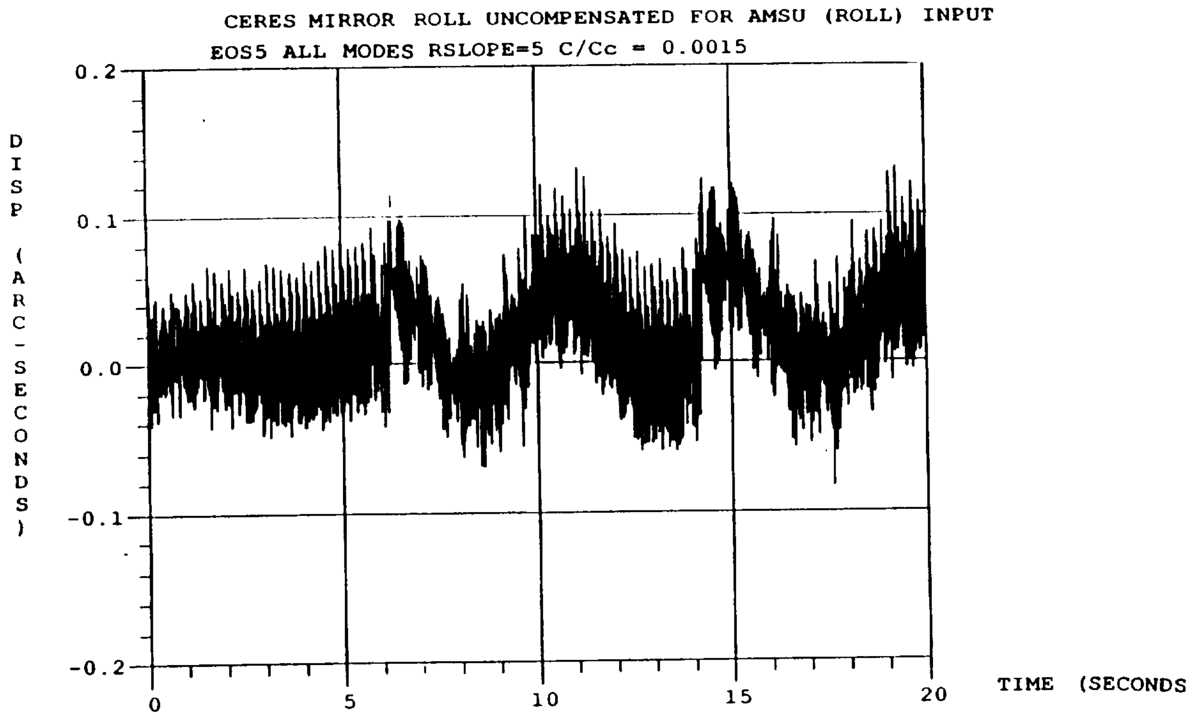

AMSU DISTURBANCE EXCITES HIGH FREQUENCY MODES

COMPENSATED CERES RESPONSE TO AMSU DISTURBANCE
RIGID BODY MODES ONLY

The jitter values are essentially the same as the baseline (uncompensated) case.. Careful observation will discern the fundamental solar array mode at approximately 0.2 Hertz (5 second period) with higher frequency components superimposed. Jitter suppression is not effective for the rigid body predictor model.

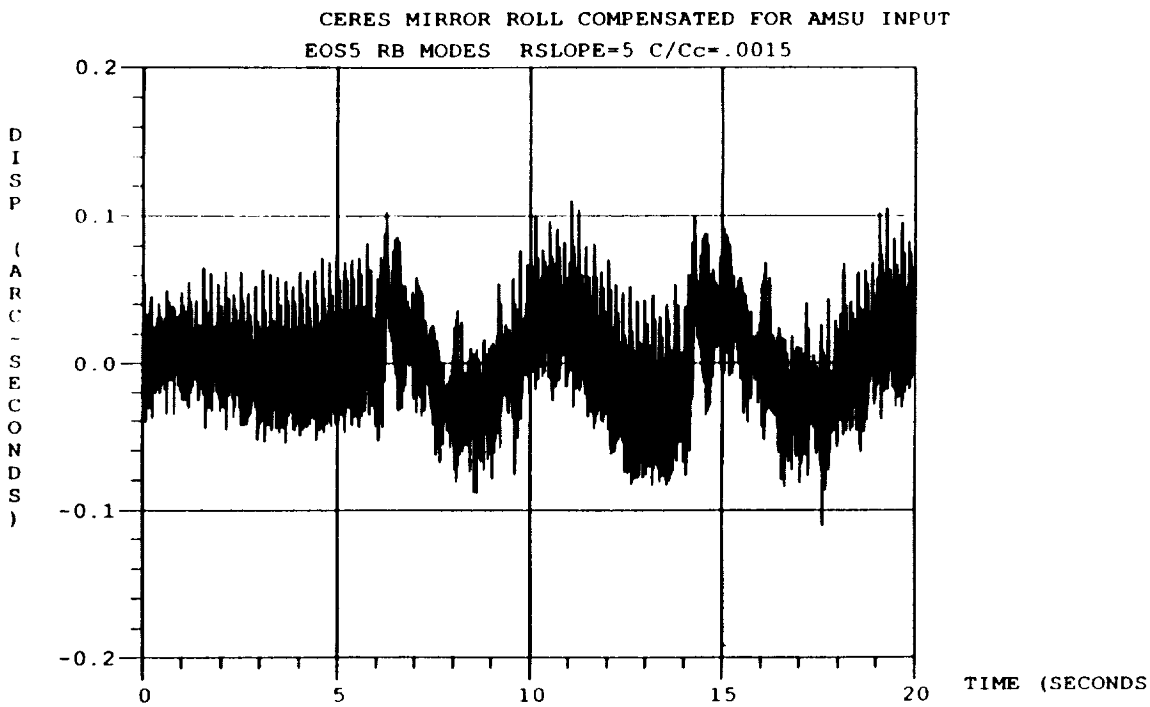

MMC WITH RIGID BODY MODES DOES NOT CONTROL JITTER
HIGH FREQUENCIES CONTRIBUTE TO JITTER

COMPENSATED CERES RESPONSE TO AMSU DISTURBANCE
RIGID BODY PLUS FLEXIBLE MODES 22, 42, 150, 153, 155

Based on a modal significance study modes 22 (at 0.208 Hz), 42 (at 1.009 Hz), 150 (at 31.629 Hz), 153 (at 33.613 Hz), and 155 (at 36.123 Hz) were seen to be significant for the AMSU - CERES interaction. These modes were included in the predictor model and resulted in some jitter reduction. The response plot on the facing page shows that the response attributable to the fundamental solar array mode has been suppressed. It is obvious, however, that the MMC technique is not as effective in reducing jitter from AMSU as compared with the reduction from the MODIS-T disturbance. The AMSU disturbs high frequency modes which are more difficult to compensate.

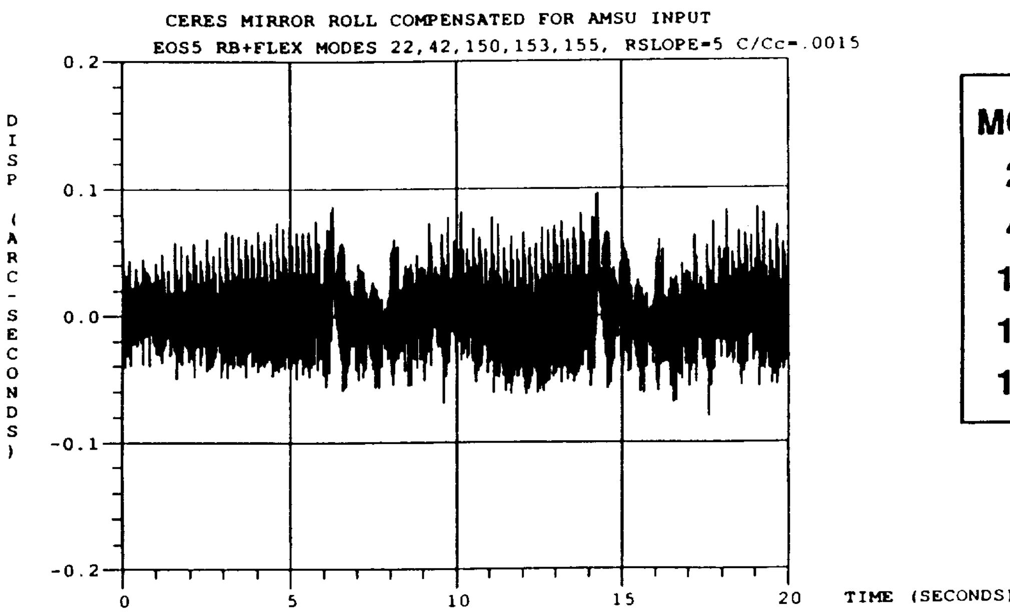

MODE	f (Hz)
22	0.208
42	1.009
150	31.629
153	33.613
155	36.123

PERFORMANCE IMPROVES WITH SUPPRESSION OF HIGHER MODES

SUMMARY TABLE OF CERES RESPONSE TO AMSU INPUT

The summary table demonstrates the less effective performance of MMC for the high frequency AMSU disturbance. Only marginal jitter reduction was achieved (a factor of 1.2) for the most sophisticated predictor model (all modes). The main reason for the poorer MMC performance can be traced to the high frequency nature of the AMSU disturbance. Further, the lag filter becomes more of a factor as the required response frequencies increase.

MODEL	JITTER IN ARC SECONDS WINDOW SIZE (SECONDS)			
	1.0	9.0	60.0	1000.0
UNCOMPENSATED	0.1928	0.2354	0.2512	0.2512
RIGID BODY MODES	0.1935	0.2311	0.2311	0.2311
RB + MODES 22 ,42,150, 153,155	0.1633	0.1766	0.1815	0.1815
RB + ALL MODES	0.1600	0.1767	0.1811	0.1811

MMC TECHNIQUE LESS EFFECTIVE FOR HIGH FREQUENCY EXCITATION

LAG FILTER SIMULATING MOTOR LAG LIMITS EFFECTIVENESS

LAG FILTER

The lag filter is present in the truth model to provide a variable and controllable source of error in the simulation. It simulates the physical behavior of an electric motor which, when given a torque command, takes some finite time to achieve the full torque value. For any time step, the relationship between the required torque and the available torque is given by Ta=Tr*(1-e**(-at)) where Ta is the torque available, Tr is the torque required (for perfect nulling), a is the time constant, and t is the time variable. The plot shows the effect of the lag filter on a step pulse. The parameter RSLOPE was varied from 1 to 5 to 10 to demonstrate the effect of this parameter on the applied torque. The RSLOPE parameter controls the rise time of the torque pulse. As the value of RSLOPE decreases the rise time increases.

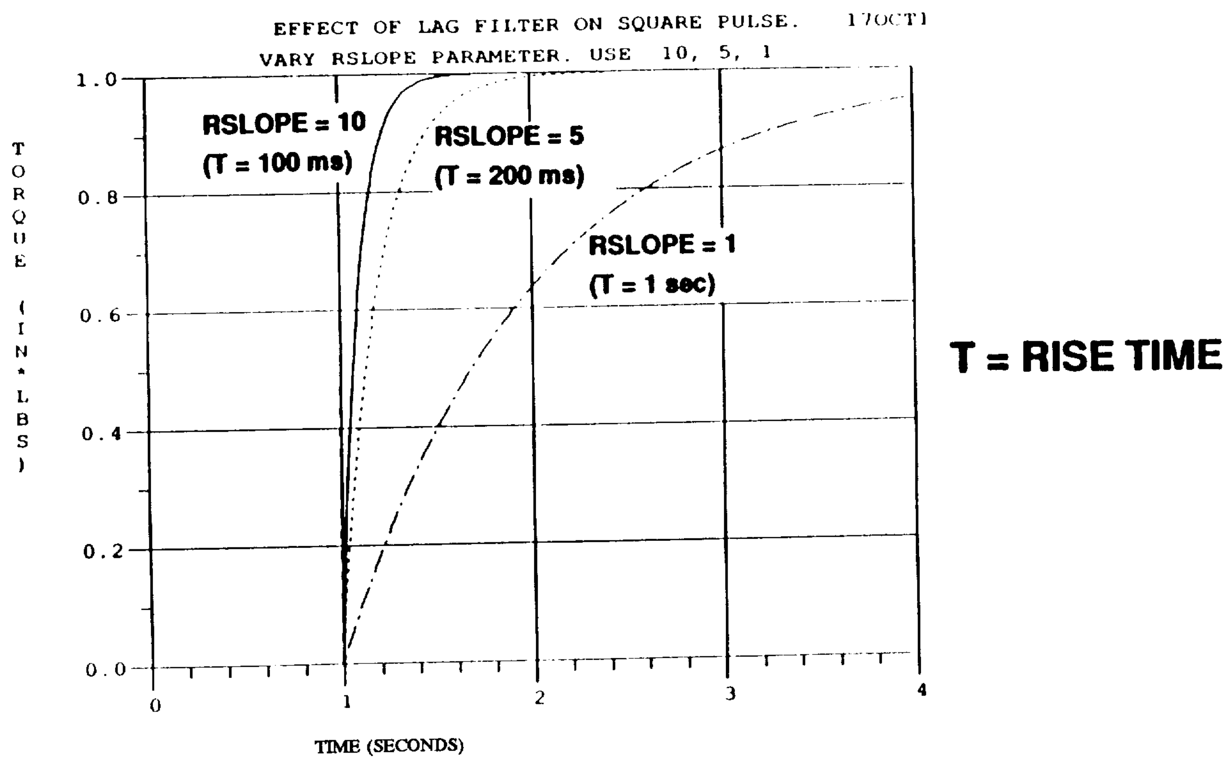

LAG FILTER
EFFECT OF LAG FILTER VARIATION ON JITTER

If the lag filter is effectively eliminated by specifying a very short time constant the jitter suppression for the AMSU disturbance will improve from a factor of 1.2 to almost 2. This is still not as good as that obtained for the MODIS-T. A full modes predictor model was run with the AMSU disturbance with the effect of the lag filter eliminated. Jitter values less than 0.1 arc seconds were obtained. Note that other sources of jitter are still present, such as compensating torque reactions.

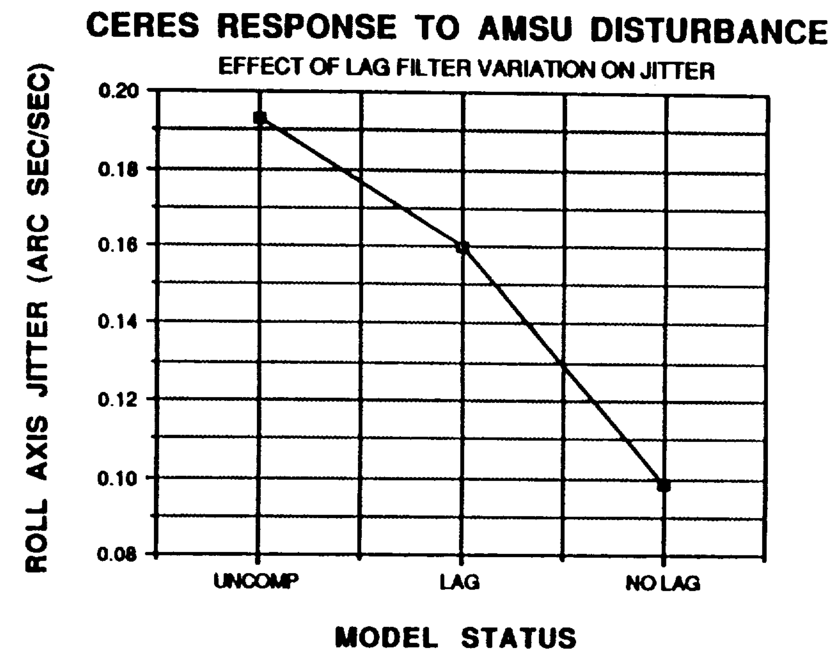

LAG PHENOMENON ADVERSELY AFFECTS JITTER COMPENSATION

MODELING UNCERTAINTIES

Although impressive jitter suppression results are predicted for the MMC technique, the question of the system's robustness remains to be explored. The results thus far have assumed a priori perfect knowledge of the important system parameters - structure natural frequencies and mode shapes, disturbance torque profiles, structural damping, sensor dynamics, and the phase relationship between the disturbance and the compensation motion. In an attempt to ascertain the effect of uncertainty of these parameters on MMC system performance a series of parametric studies was conducted.

- **COMPENSATION IS EFFECTIVE WITH "PERFECT" KNOWLEDGE**

- **EVALUATION OF EFFECTIVENESS OF MMC SYSTEM WITH UNCERTAINTIES:**

  - **STRUCTURAL DYNAMIC PROPERTIES**

    FREQUENCY

    DAMPING

  - **ACTUATOR RESPONSE UNCERTAINTIES**

    LAG

FREQUENCY SENSITIVITY
COMPENSATED CERES RESPONSE TO MODIS-T INPUT

There is an inherent limit in the accuracy to which structural normal modes can be predicted. The uncertainties in natural frequency between the predicted and actual values will affect MMC system performance. The nature of this MMC simulation allows us to explore the effect resonant frequency uncertainty will have by using a different natural frequency in the predictor model from that used in the truth model.

The plot shows the effect on the CERES response to MODIS-T disturbance of varying the predicted natural frequency of the fundamental solar array mode from its nominal value (used in the truth model) of 0.208 Hertz. The plot shows that for a +/-10 % variation (0.187 Hertz to 0.229 Hertz) the compensated jitter performance is substantially worse than if no compensation system were present. This is due to the phasing of the input and the response, which, for slight differences in frequency between the truth and predictor model, will result in the well known beating phenomenon as the input and response move in an out of phase, alternately adding constructively and destructively. In fact, the plot indicates that the MMC performance is extremely sensitive to variations in frequency between the predictor model and the truth model. Even a +/- 1 % variation is inadequate. This betrays a serious weakness in the system, since structural modes are predicted, at best, to within 5 %. Thus we conclude that, for cases where the flexible response is large, the feasibility of the MMC system depends heavily upon our knowledge of the structural natural frequencies which must be known exactly if any benefit is to be realized from this technique.

The effect of frequency uncertainty on stability is also demonstrated in this plot. The curve for stability displays the same behavior as the jitter curve, but is always below the uncompensated value; thus stability is always improved by the action of the MMC system regardless of reasonable frequency error.

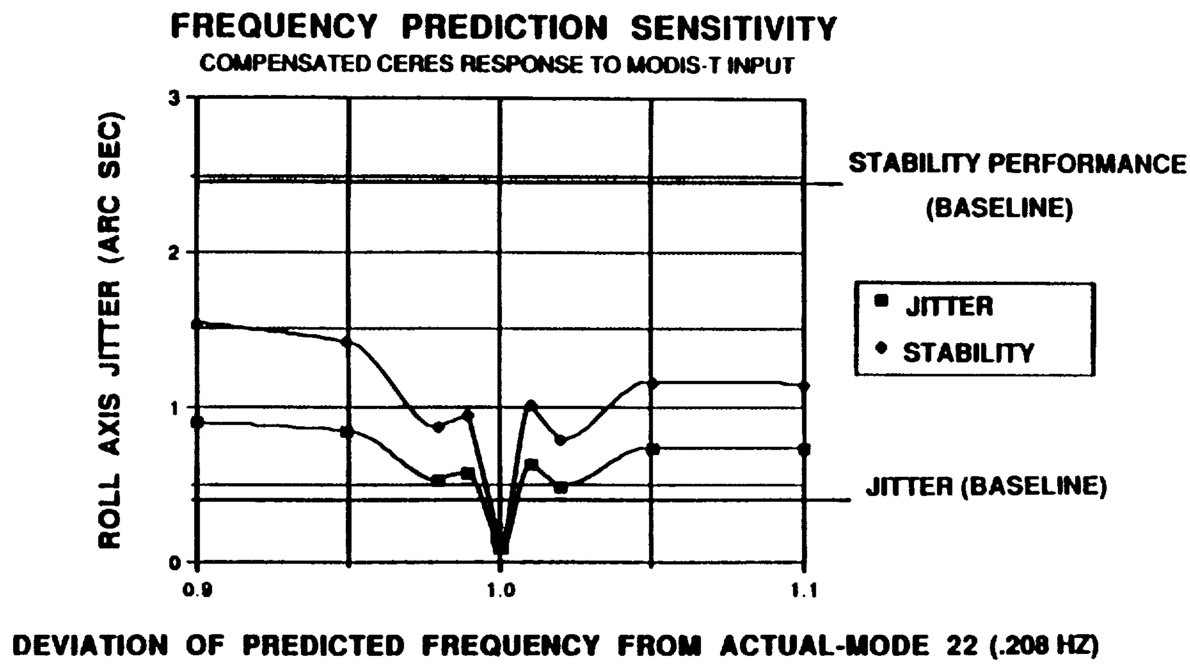

- **EFFECTIVENESS OF JITTER COMPENSATION SENSITIVE TO FREQUENCY KNOWLEDGE**
- **STABILITY PERFORMANCE IMPROVEMENT ACHIEVABLE WITH FREQUENCY ERRORS**

FREQUENCY SENSITIVITY
COMPENSATED CERES RESPONSE TO AMSU INPUT

The plot further explores the sensitivity of the MMC technique to the structural natural frequency parameter. A +/- 10 % variation of predicted natural frequency is again evaluated, this time on those modes significant to the CERES response to the AMSU input (modes 22 (at 0.208 Hz), 42 (at 1.009 Hz), 150 (at 31.629 Hz), 153 (at 33.613 Hz), and 155 (at 36.123 Hz)). The variation was imposed on all five significant modes simultaneously.

We note immediately that the curve is broader in the region of interest about the nominal frequencies, thus indicating less sensitivity to frequency uncertainty. The high frequency nature of the AMSU disturbance is largely responsible for this behavior. At the higher frequencies the damping present has more effect and damps out the higher modes proportionally more rapidly since it operates on more cycles over a shorter period of time. The broadening of the sensitivity curve is analogous to the broadening of a response curve with increasing damping of a single degree of freedom harmonic oscillator around resonance.

Stability again is generally improved for all reasonable values of frequency, but is marginal at differences greater than 5%.

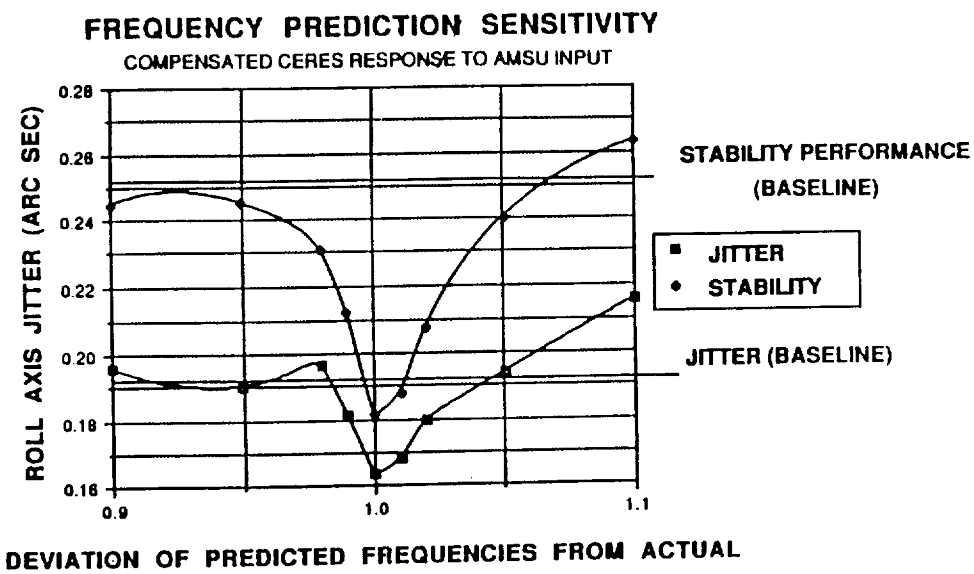

- JITTER REDUCTION NOT AS EFFECTIVE FOR AMSU
- JITTER COMPENSATION NOT AS SENSITIVE TO FREQUENCY ERROR

DAMPING PARAMETRIC STUDY

The damping is another parameter which affects MMC performance and is difficult to predict. Thus it was necessary to characterize the behavior of the system with variations in damping, first in its effect on the frequency study previously described.

The damping in both the predictor model and truth model, applied as modal damping, identical for all modes, was varied from the baseline value of 0.0015 C/Cc through 0.005, 0.015, and 0.03 C/Cc. Simultaneously, the frequency of the fundamental solar array mode was varied in the predictor model while held constant in the truth model as in the previous analysis. The family of curves which resulted is shown for the CERES response to the MODIS-T disturbance.

We immediately recognize the baseline run, representing light damping at 0.0015 C/Cc, with its characteristic narrow band and poor jitter compensation with any frequency error. As the system damping increases we note the broadening of the curves as expected, indicating less sensitivity to frequency error with increasing damping. In addition, the overall jitter level decreases dramatically with increasing damping, until, at the heavily damped level of 0.03 C/Cc, the jitter performance is superior to the uncompensated baseline response over the entire +/- 10 % range variation. This is also true for the damping value of 0.015 C/Cc.

Thus we see dramatically the advantage obtained by increased damping, indicating that it would be worthwhile to include passive damping in the system to enhance system performance and further suppress jitter effects.

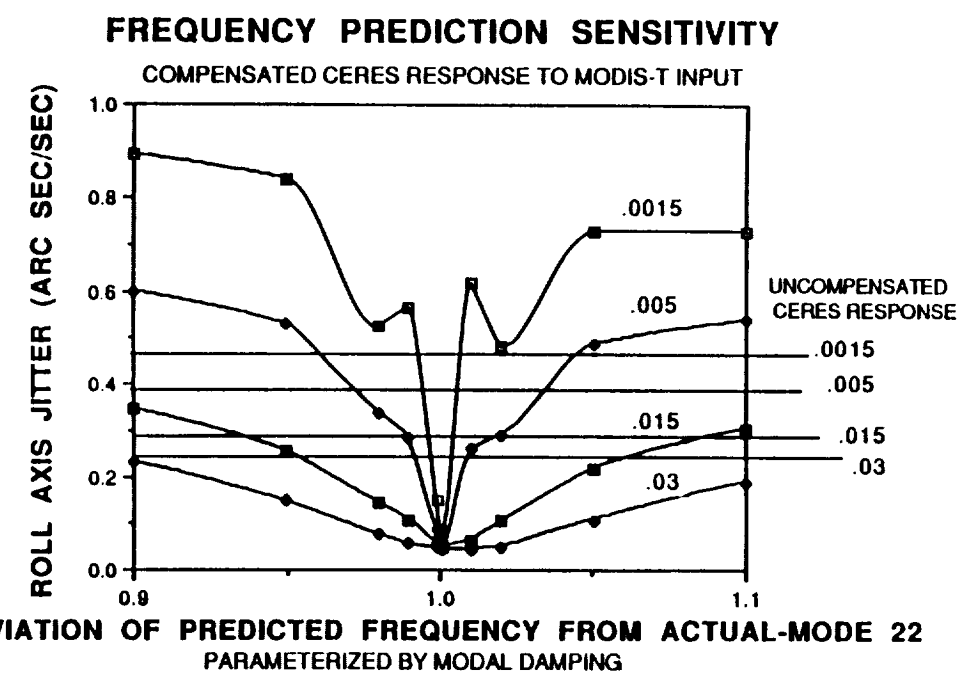

- **DAMPING REDUCES ERROR SENSITIVITY**
- **DAMPING EFFECTIVELY SUPPRESSES JITTER**

DAMPING SENSITIVITY

Further damping studies explored the effect of predicted damping differing from actual damping. The effect was evaluated by varying the damping in the predictor model from the value used in the truth model. This was performed for three different damping baseline values producing the family of curves shown in the plot below.

Each curve represents a different baseline modal damping value used in the truth model, as indicated by the curve label of 0.0015, 0.005, 0.015 C/Cc. The curves were generated by varying the predictor model damping among the values 0.0015, 0.005, 0.015, and 0.03 C/Cc and plotting the maximum jitter.

Trends revealed by the exercise show the expected jitter decrease with increasing damping, consistent with previous work. Note that as we under-predict or over-predict the damping the jitter control performance degrades although not as severely as with frequency variation. The predicted jitter is below the uncompensated baseline values for all reasonable damping variations, indicating the less critical nature of the damping parameter with regard to jitter performance.

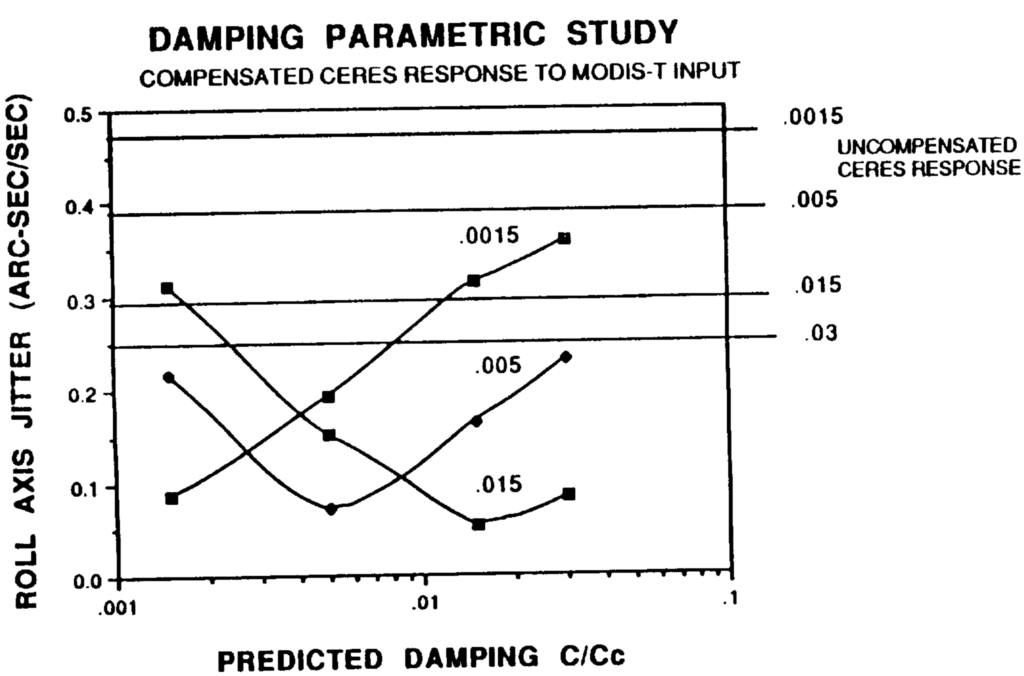

MMC EFFECTIVENESS NOT AS SENSITIVE TO DAMPING PREDICTION ERRORS

JITTER SENSITIVITY TO LAG FILTER

As described previously, a lag filter was incorporated in the truth model to provide a source of variable, controllable error. The lag filter simulates the actual response of a motor actuator by attenuating the torque required to provide perfect compensation of the subject mirror sensor.

In this sensitivity study the lag filter time constant was varied from 2 seconds through 67 milliseconds, simulating a decreasing motor response time. The resulting curve depicts the effect of lag filter variation on roll axis jitter of the CERES response to the AMSU disturbance. Note that the jitter approaches a limiting value as the response time of the motor decreases, indicating other sources of error as described before. Note that the predictor model is the AMSU significant mode subset of modes 22, 42, 150, 153, and 155. This is no doubt a partial cause for the limited jitter reduction seen in the plot.

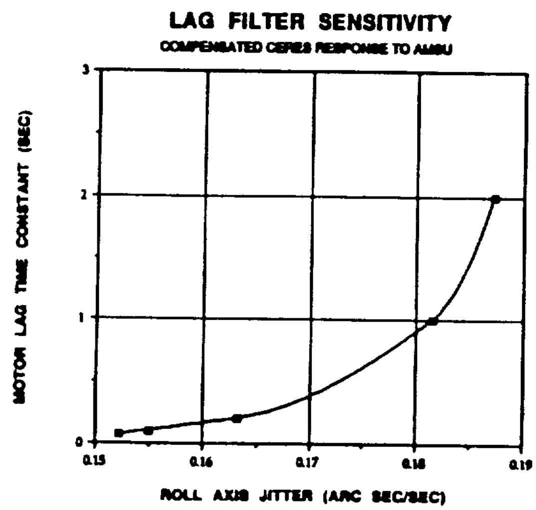

INCREASING LAG CONSTANT CORRESPONDS TO DECREASING RESPONSE TIME

JITTER APPROACHES LIMITING VALUE AS LAG CONSTANT INCREASES

MIRROR INERTIA STUDY

Of interest to the study was the effect of larger mirrors on MMC system performance. The effect of larger mirrors was explored by examining the CERES response to both MODIS-T and AMSU inputs for increasing CERES mirror roll axis mass moment of inertia.

The baseline inertia was varied by factors of 2x, 5x, 10x, 20x, and 50x in a series of runs where maximum jitter was calculated for each disturbance source. As the mirror inertia is increased, the larger secondary torques required for the MMC correction eventually override the baseline disturbances. For MODIS-T this is seen to happen when the mirror inertia is increased by a factor greater than 2. This is demonstrated in the plot below.

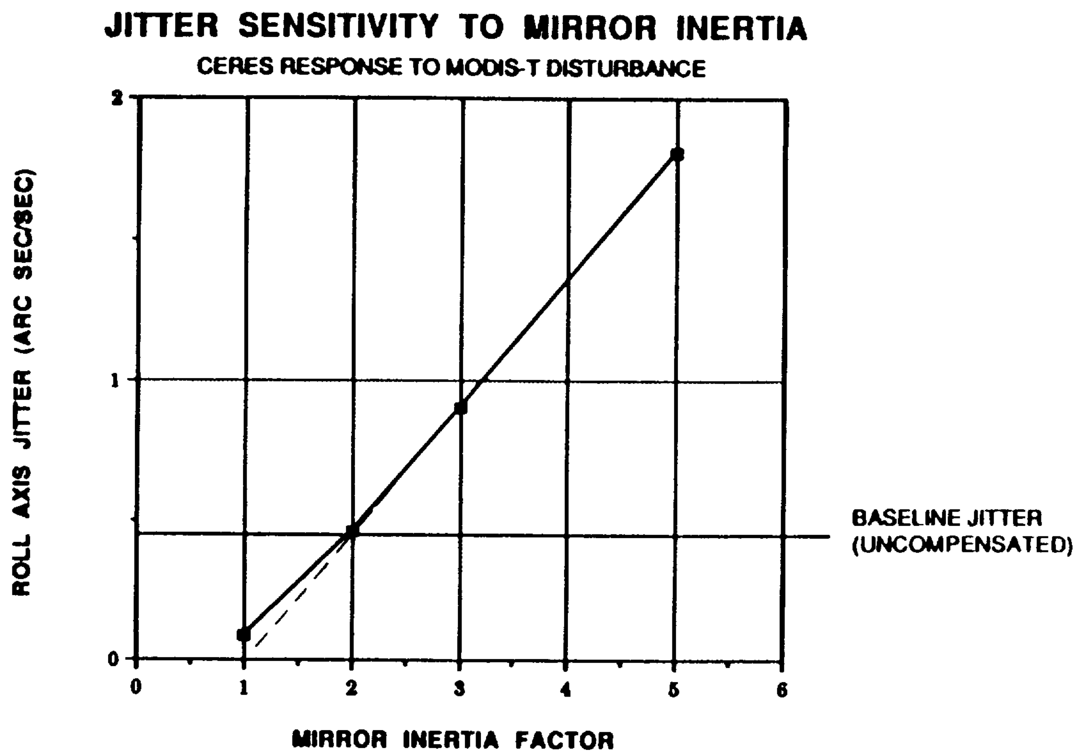

JITTER INCREASES WITH MIRROR INERTIA

MIRROR INERTIA STUDY
SUMMARY TABLE OF CERES RESPONSE TO AMSU INPUT

The summary table displays the information obtained in the mirror inertia study for jitter and stability behavior of the CERES for the AMSU disturbance.

MODEL	JITTER IN ARC SECONDS WINDOW SIZE (SECONDS)			
	1.0	9.0	60.0	1000.0
BASELINE AMSU	.1633	.1766	.1815	.1815
2 X INERTIA	.1973	.2202	.2355	.2371
5 X INERTIA	.3627	.4348	.5585	.5698
10 X INERTIA	.6595	.8127	1.115	1.136
20 X INERTIA	1.241	1.585	2.231	2.269
50 X INERTIA	3.061	3.937	5.616	5.735

MIRROR INERTIA STUDY
SUMMARY TABLE OF CERES RESPONSE TO MODIS-T INPUT

The summary table of complete CERES response to the MODIS-T disturbance for the mirror inertia study, including both jitter and stability data in tabular format.

MODEL	JITTER IN ARC SECONDS WINDOW SIZE (SECONDS)			
	1.0	9.0	60.0	1000.0
BASELINE MODIS-T	.0866	.1438	.1492	.1492
2 X INERTIA	.4613	.9755	1.911	2.467
5 X INERTIA	1.809	3.903	7.658	9.865
10 X INERTIA	4.066	8.796	17.25	22.21
20 X INERTIA	8.594	18.59	36.44	46.89
50 X INERTIA	22.17	47.97	94.00	>100

MULTIPLE DISTURBANCES
UNCOMPENSATED CERES RESPONSE TO AMSU AND MODIS-T DISTURBANCE

Time history plot showing the CERES response to AMSU and MODIS-T disturbances occurring simultaneously. The combined response is the superposition of the individual responses, as can be readily observed in the plots below.

UNCOMPENSATED RESPONSE TO AMSU AND MODIS-T DISTURBANCE

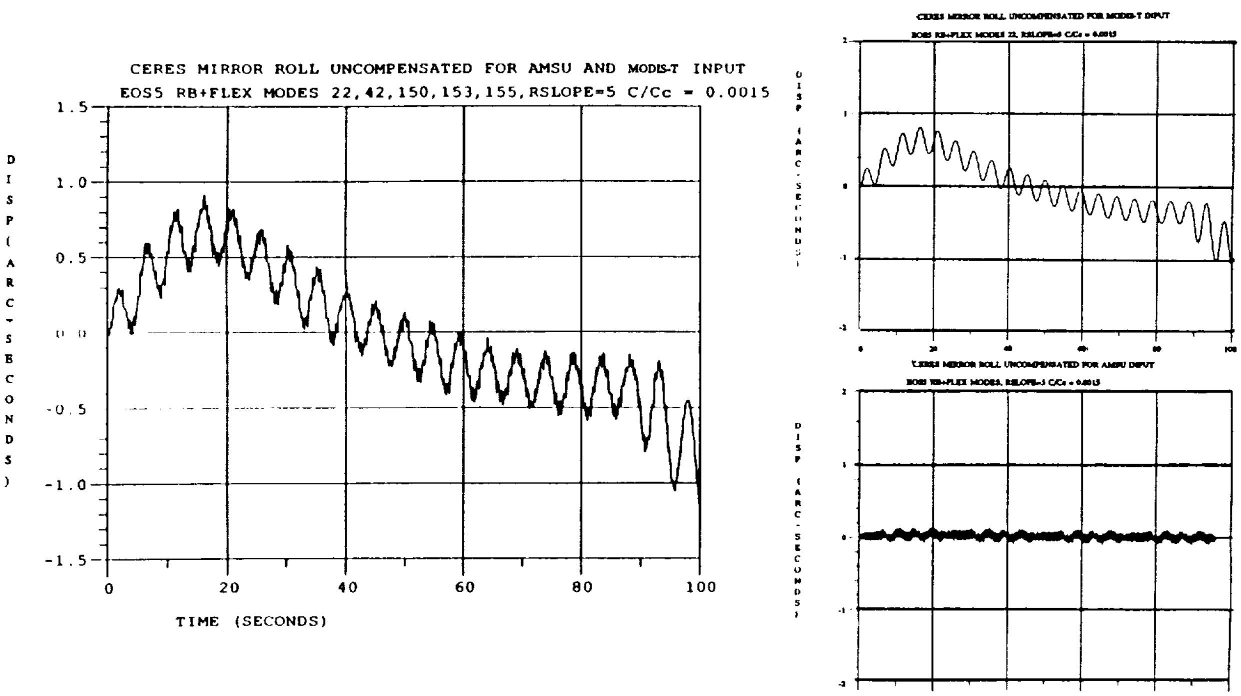

COMBINED RESPONSE IS SUPERPOSITION OF INDIVIDUAL RESPONSES

MULTIPLE DISTURBANCES
COMPENSATED CERES RESPONSE TO AMSU AND MODIS-T DISTURBANCE

As seen in the plots below, the MMC logic works effectively for the case when both disturbance sources are applied at the same time. The residual jitter value for combined torques with compensation is somewhat lower than the two individual compensated responses.

COMPENSATED RESPONSE TO AMSU AND MODIS-T DISTURBANCE

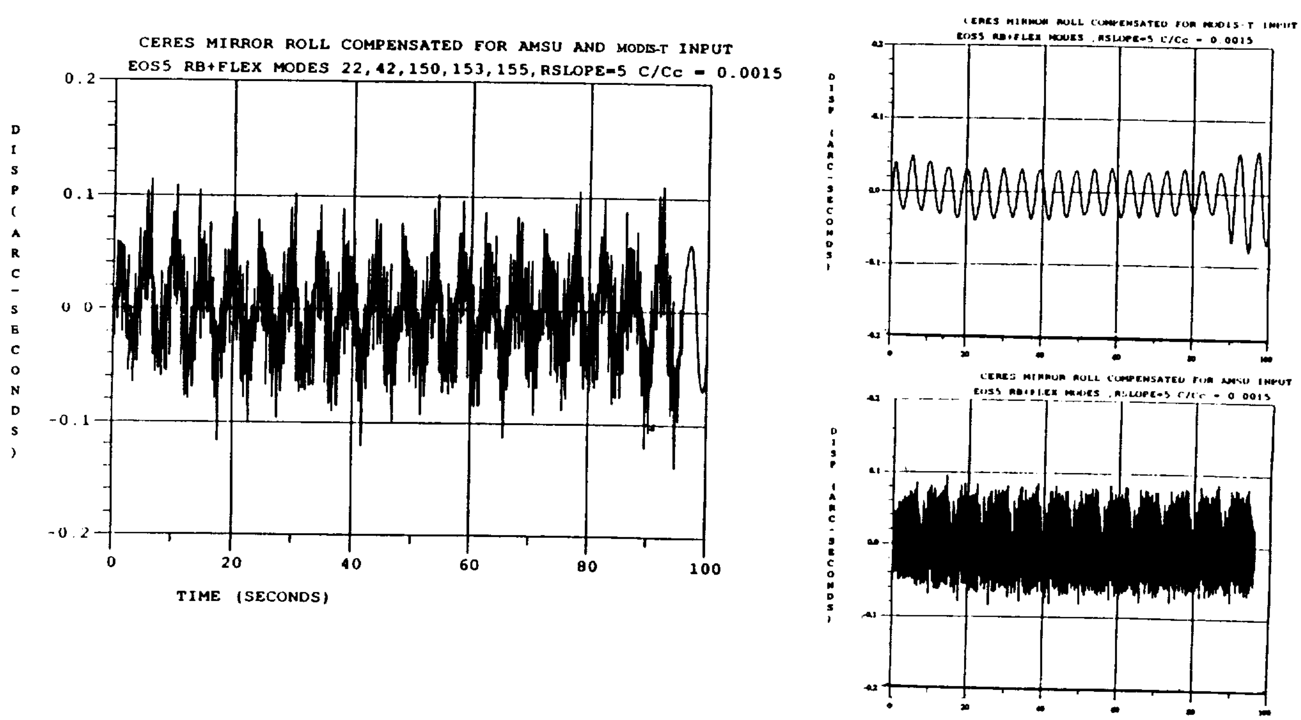

SUPERPOSITION OF COMPENSATED RESPONSE TO TWO DIFFERENT SOURCES

MULTIPLE DISTURBANCES

Graphic display of CERES roll axis jitter response due to multiple simultaneous sources (AMSU plus MODIS-T) shows that the jitter is not the sum of the individual jitter values. This is because the maximum jitter value does not occur at the same time for each disturbance response. Note that the jitter is calculated by a sampling window which moves along the time axis taking the maximum peak to peak difference between the response values within the window. The first three bars of the plot below compare the uncompensated response for AMSU disturbance alone, the combination of AMSU and MODIS-T, and the response to MODIS-T alone. The next three bars display the same information for the compensated CERES response (the MMC system active).

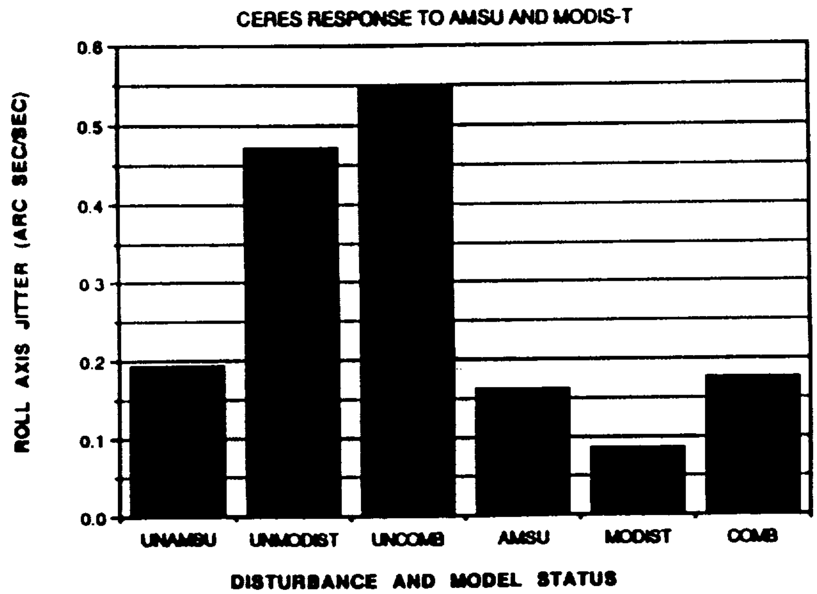

KEY

UNAMSU - UNCOMPENSATED JITTER FROM AMSU

UNMODIST - UNCOMPENSATED JITTER FROM MODIS-T

UNCOMB - COMBINATION OF UNCOMPENSATED JITTER

AMSU - JITTER FROM AMSU WITH MMC

MODIST - JITTER FROM MODIS-T WITH MMC

COMB - COMBINATION OF JITTER WITH MMC

MMC LOGIC EFFECTIVE FOR MULTIPLE DISTURBANCES

MLS SCAN 3 DISTURBANCE TORQUE PROFILE

The MMC technique was applied to suppress disturbances from the MLS instrument, which is currently on the UARS, and is well known as a pernicious source of jitter.

The torque profile is displayed below, and consists of a number of forward torque pulses, each of which rotates a scanning mirror about the spacecraft roll axis 0.05 degrees. Two return pulses follow the forward pulse train. The return profile was split into two identical parts as a result of a previous UARS disturbance torque analysis which showed high amplitude residual vibrations at the completion of each MLS scan due to return pulse excitation of the UARS solar array. The second pulse is timed to cancel the UARS solar array excitation, which yielded a 75 % reduction in the solar array free vibration when compared with the effects of a single return pulse. The MLS torque profile was applied to the EOS in this study without consideration to the EOS solar array mode.

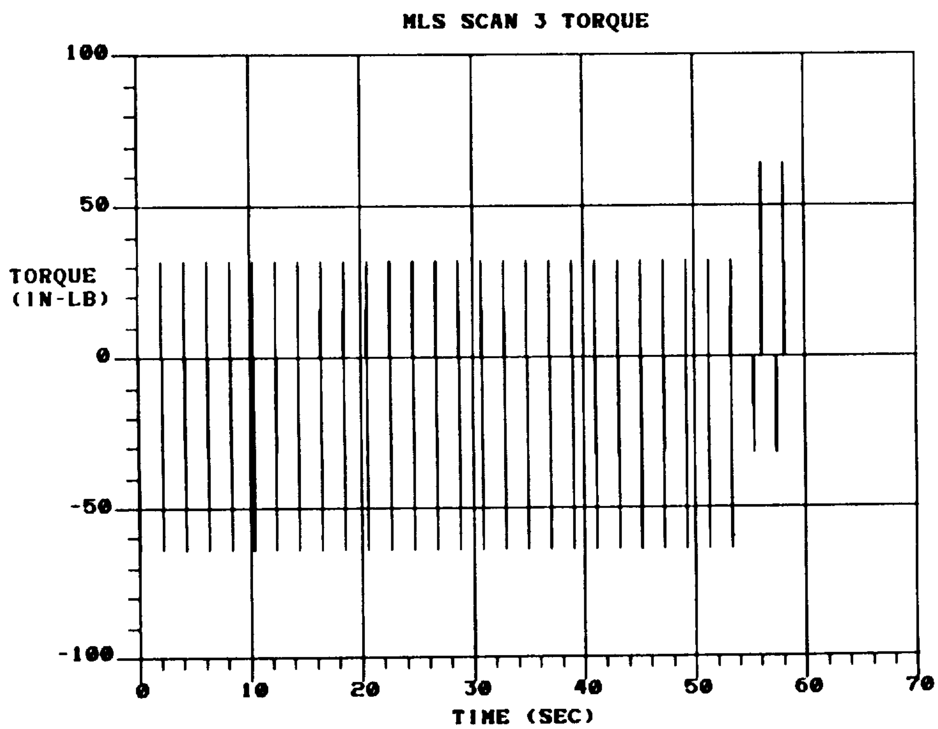

DOUBLE RETURN PULSE IMPLEMENTED TO REDUCE LARGE JITTER RESPONSE

UNCOMPENSATED CERES BASELINE RESPONSE TO MLS

The MLS disturbance excites both high and low frequency responses, as evidenced in the plot below. The forward pulse train excites the high frequency components, as seen in the plot from time zero to approximately 55 seconds, at which point the double return pulse excites the lower frequency modes, especially the fundamental solar array mode. Significant jitter results from the MLS disturbance.

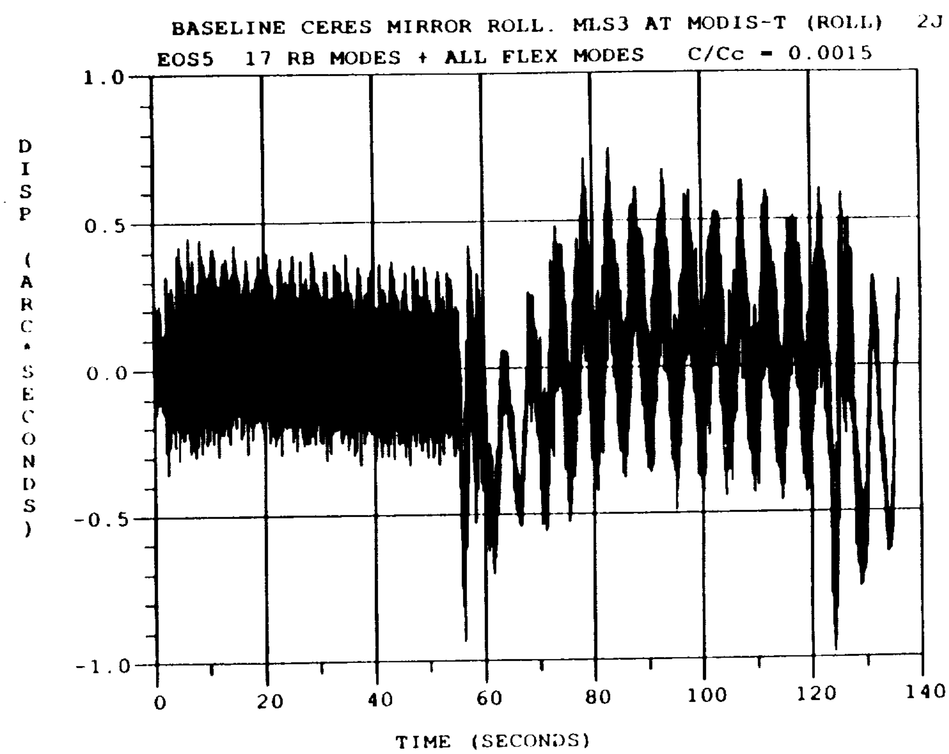

MLS EXCITES BOTH LOW AND HIGH FREQUENCY MODES

COMPENSATED CERES RESPONSE WITH RIGID BODY MODES ONLY IN PREDICTOR MODEL

Application of MMC with a primitive predictor model consisting only of the rigid body and gimbal modes proved ineffective at jitter reduction, as seen below. Jitter values actually increased slightly, due to lag filter and reverse torque error effects. Clearly a more sophisticated predictor model is required for effective jitter suppression.

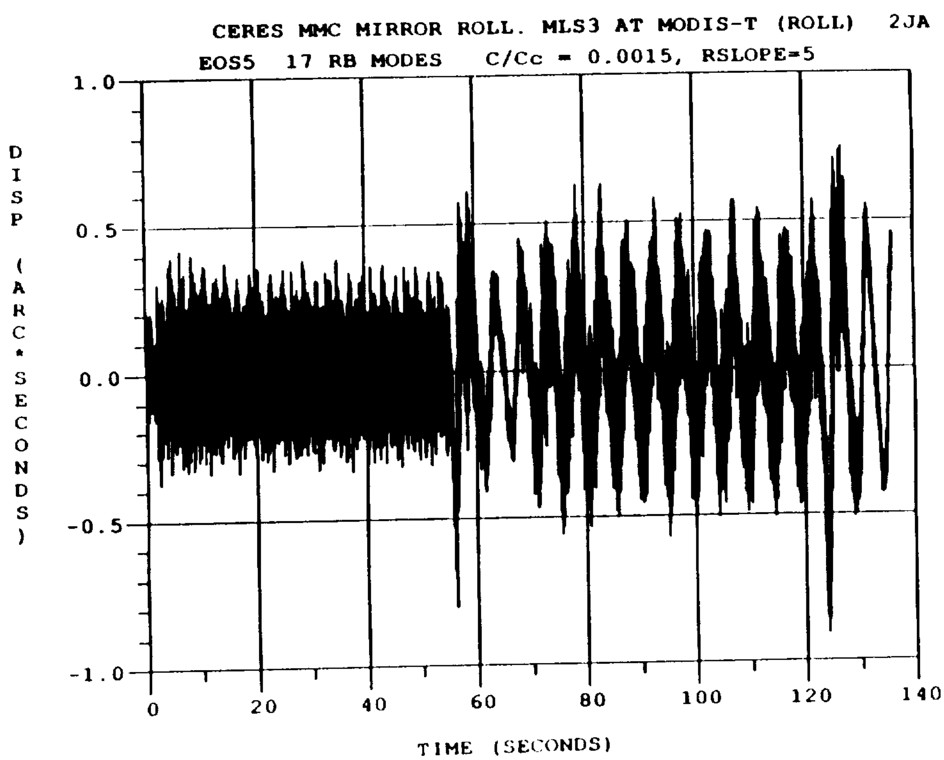

RIGID BODY PREDICTOR MODEL NOT EFFECTIVE FOR JITTER SUPPRESSION

COMPENSATED CERES RESPONSE
WITH RIGID BODY MODES PLUS FUNDAMENTAL SOLAR ARRAY MODE
IN PREDICTOR MODEL

The degree of sophistication of the MMC predictor model was increased by including the fundamental solar array mode along with the rigid body modes. The response plot below shows some jitter reduction with especially effective elimination of the solar array response as expected. The actual reduction factor for jitter is 1.5 for this model.

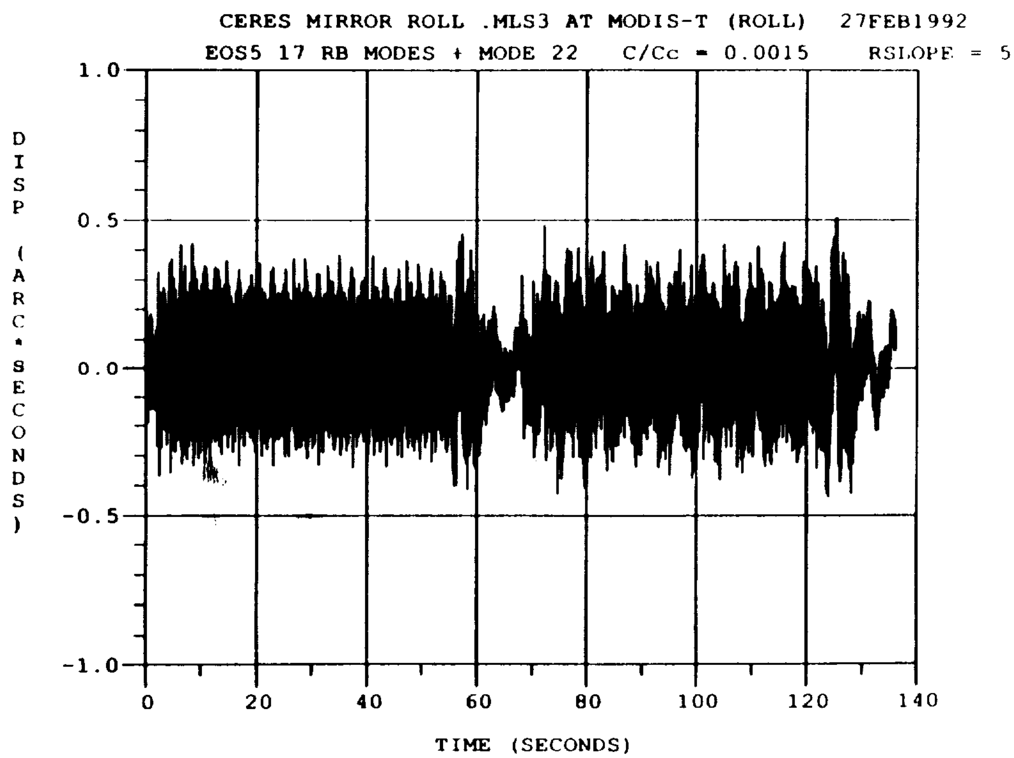

MMC EFFECTIVENESS IMPROVES WITH ADDITION OF FLEXIBLE MODE

COMPENSATED CERES RESPONSE WITH ALL FLEXIBLE MODES

The use of all flexible modes with the rigid body modes in the predictor model shows marginal improvement over the previous model with the fundamental solar array mode as the only flexible mode. A jitter reduction factor of 1.6 was achieved. No doubt a modal significance study would reveal a subset of flexible modes which would produce an equivalent jitter reduction to that achieved by the use of all the flexible modes, as seen previously in the AMSU disturbance case. Again, high frequency disturbances prove difficult for the MMC to suppress effectively given the limitations and assumptions of the study with regard to lag and reverse torque error.

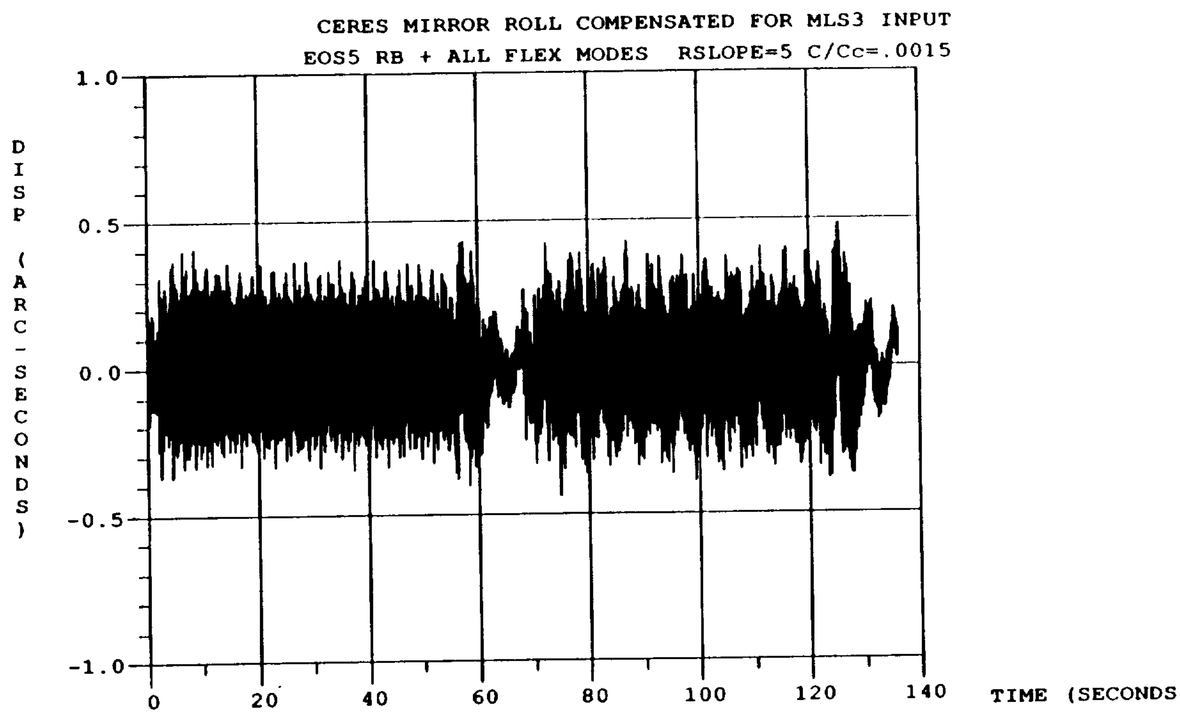

BEST MMC PERFORMANCE ACHIEVED WITH ALL FLEXIBLE MODES

COMPENSATED CERES RESPONSE WITH ALL FLEXIBLE MODES
NO LAG

As expected, when the error due to motor lag is removed the MMC performance improves and the jitter is further reduced. Note particular improvement in the response caused by the return pulse.

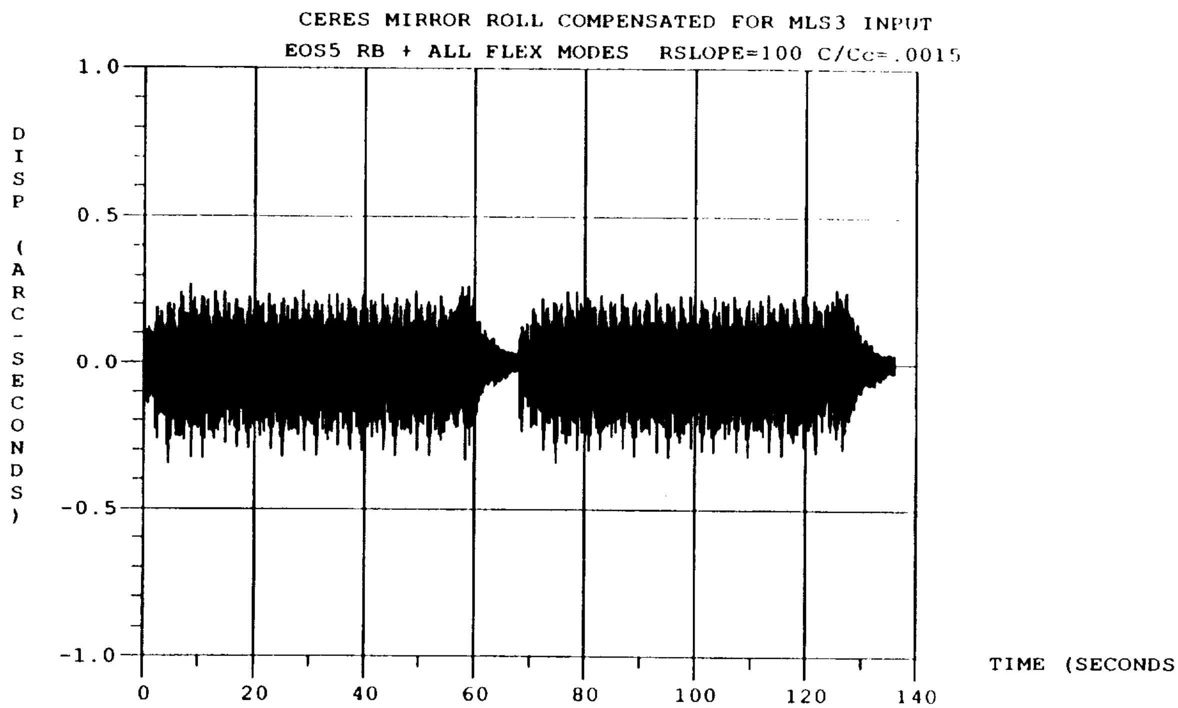

RESPONSE WITH NO LAG PROVIDES IDEALIZED COMPARISON

SUMMARY TABLE OF CERES RESPONSE TO MLS DISTURBANCE

The chart below summarizes the jitter reduction and stability performance for the CERES response to the MLS disturbance for various predictor models. Comparison with the baseline predictions shows modest jitter reduction, with a maximum factor of 1.6 realized. Stability results are also lackluster, with a maximum reduction factor of 1.87 seen.

MODEL STATUS	JITTER IN ARC SECONDS WINDOW SIZE (SECONDS)			
	1.0	9.0	60.0	1000.0
UNCOMPENSATED	1.367	1.588	1.731	1.731
RIGID BODY MODES	1.387	1.663	1.663	1.663
RB + FUNDAMENTAL S/A	0.901	0.951	0.951	0.951
RB + ALL FLEX MODES	0.835	0.868	0.925	0.925
RB + FLEX MODES NO LAG	0.601	0.619	0.619	0.619

HIGH FREQUENCY CONTENT OF MLS DISTURBANCE LIMITS EFFECTIVENESS OF JITTER SUPPRESSION TO A FACTOR OF 1.6

FEEDBACK

In order to explore the possibility of utilizing a feedback control scheme as opposed to the MMC system thus far described, a simplified feedback control concept was studied.

Although there is no doubt that a classic sophisticated feedback control system could be developed to suppress instrument jitter, the intent of this study is to explore less costly alternatives which could prove effective in jitter control and suppression. Thus a feedback control system using information from sensors already on the platform for other purposes was proposed.

In this highly idealized approach it is assumed that gyros at the NAVBASE can provide rotational acceleration data about all three axes. The signals from these gyros is assumed to be free of noise, furthermore, no sampling rate limits are present.

The chart below displays a diagram of the logic steps which are followed in this NAV BASE feedback algorithm.

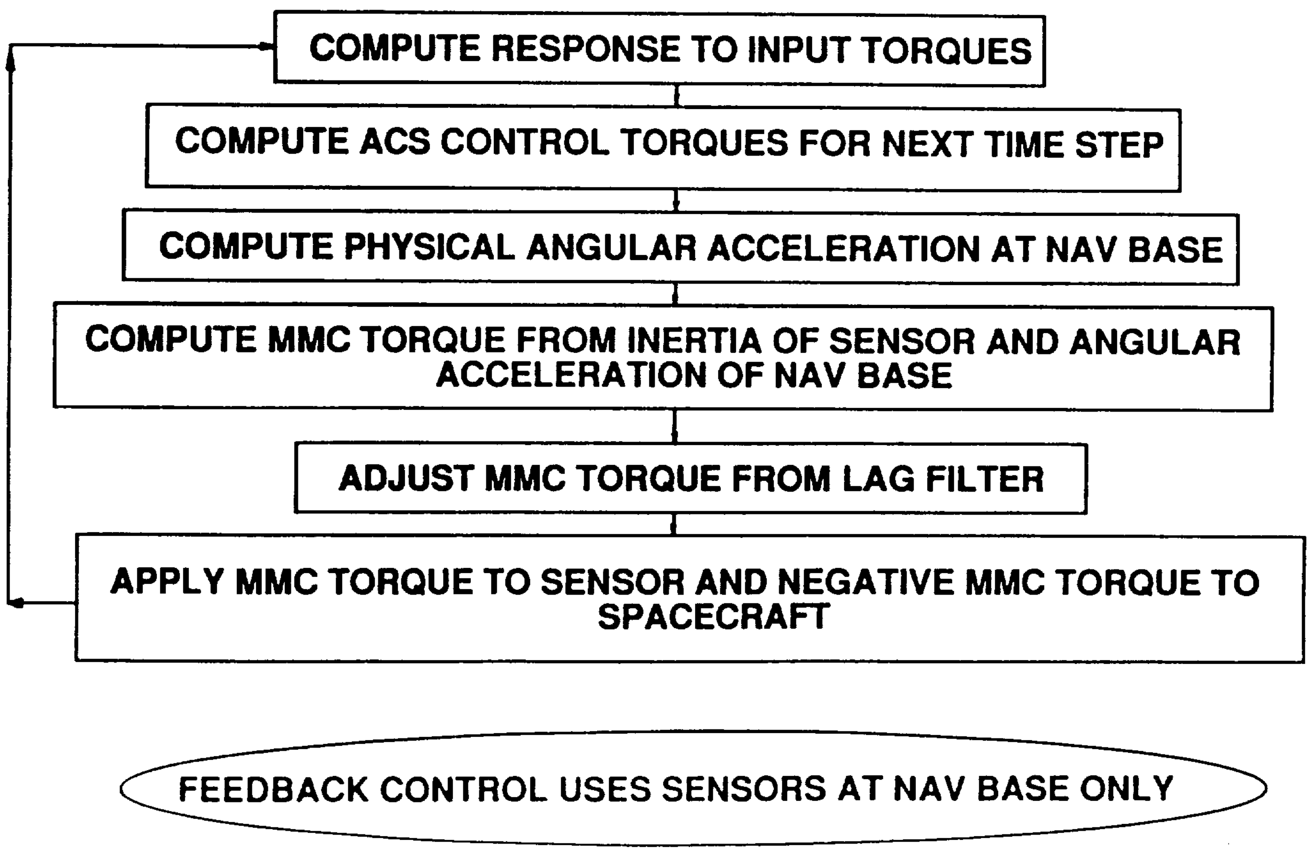

FEEDBACK

In order to provide a fair comparison between the MMC technique considered in this study and the NAV BASE feedback system, the compensated jitter response of the CERES to the MODIS-T input was calculated with the MMC technique. The MMC technique is employed in an ideal case eliminating error sources due to frequency and damping, and matching the lag effects between it and the NAV BASE system. The secondary reaction torques are present as an error source, however, since the MMC system does not take these into account when it makes its response predictions.

The chart below shows the jitter time history of the compensated CERES response to the MODIS-T disturbance calculated via the MMC technique. This plot forms the baseline for comparison with the NAV BASE feedback system, shown on the next viewgraph. The predictor model consists of 17 rigid body and gimbal modes plus the fundamental solar array mode. It must be emphasized that this is an unrealistically ideal case presented for comparison purposes only.

BASELINE MMC FOR COMPARISON WITH FEEDBACK
COMPENSATED CERES RESPONSE TO MODIS-T INPUT
17 RIGID BODY MODES PLUS FUNDAMENTAL SOLAR ARRAY MODE

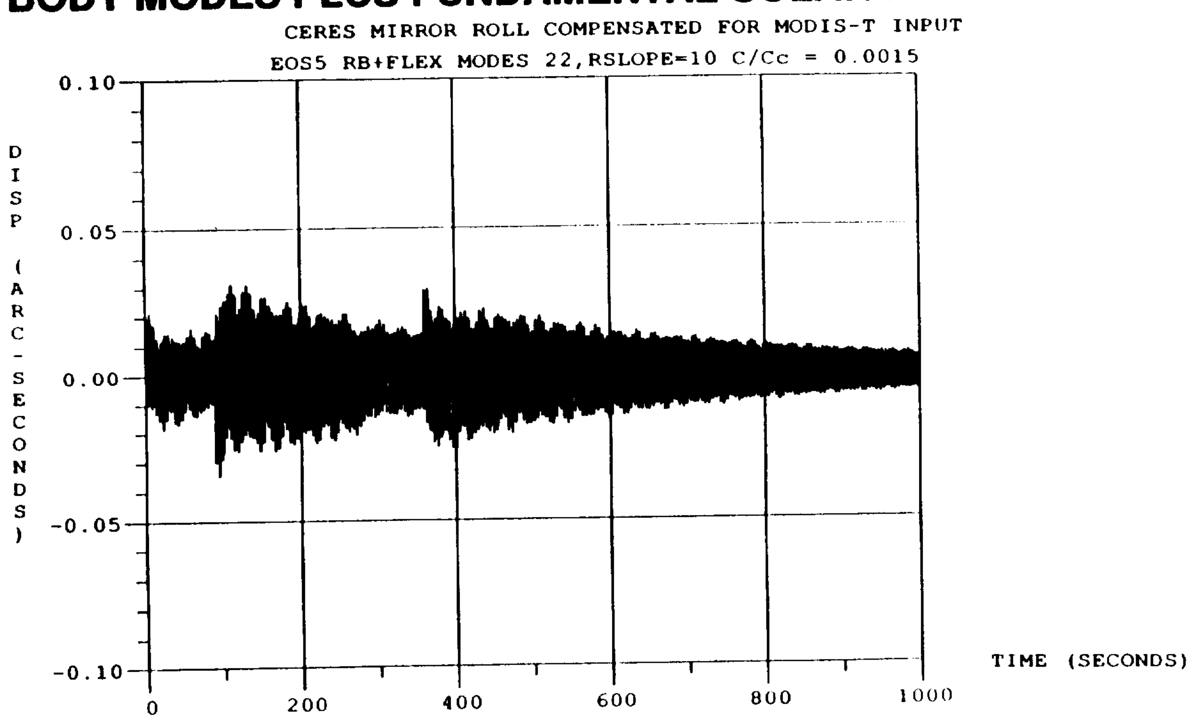

EFFECTIVE JITTER COMPENSATION WITH PERFECT KNOWLEDGE

The chart below shows the effectiveness of the NAV BASE feedback system for mirror motion compensation. The jitter for the CERES response to the MODIS-T input is displayed. Note that the models for the MMC system and NAV BASE feedback system are of the same degree of sophistication, both featuring 17 rigid body and gimbal modes plus the fundamental solar array mode. In addition, roughly the same error due to lag is present in both models. Further equivalent idealizations were made for both models as outlined previously.

Under these ideal conditions the NAV BASE feedback system is effective in jitter control, showing a substantial jitter reduction over the uncompensated baseline. The MMC system shows very similar effectiveness.

COMPENSATED CERES RESPONSE TO MODIS-T DISTURBANCE
NAV BASE FEEDBACK SYSTEM WITH SOLAR ARRAY MODE

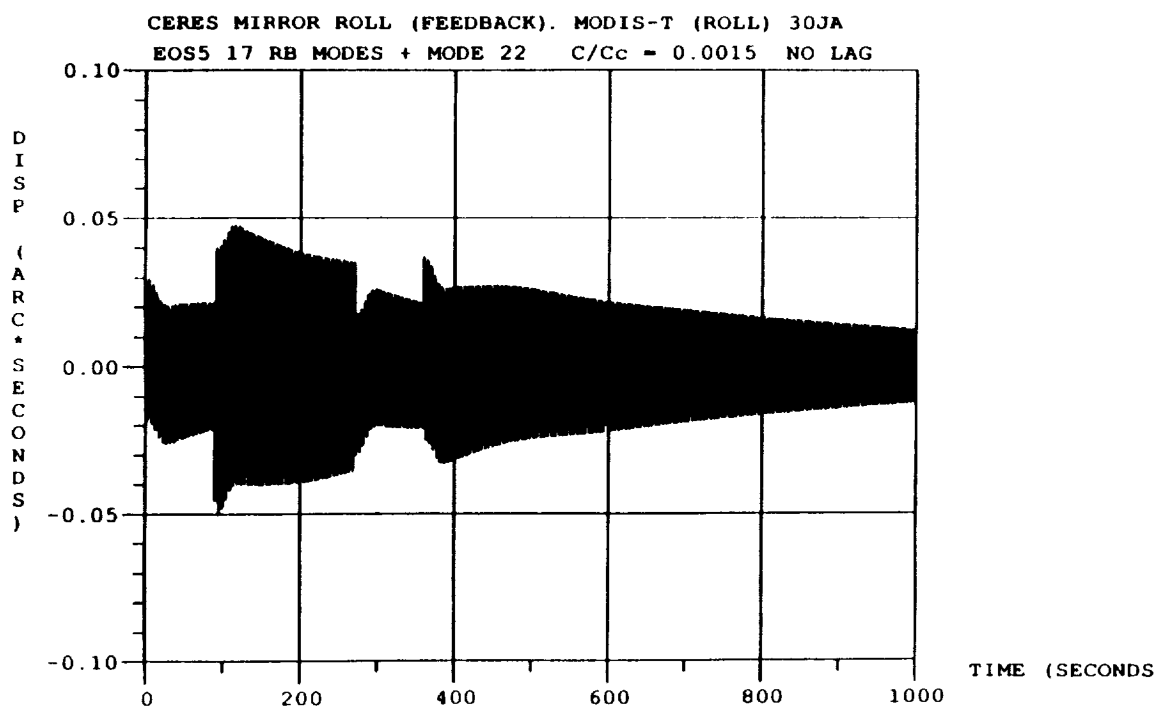

EFFECTIVE COMPENSATION POSSIBLE SIMILAR TO MMC

FEEDBACK

The chart below provides direct numerical comparison between the uncompensated jitter, the jitter with MMC for a lag constant of 10, and the jitter for the idealized NAV BASE feedback system. All jitter values refer to CERES roll response due to MODIS-T disturbance. Stability values are presented as well. Again, the numbers show that the NAV BASE feedback system provides effective jitter control compared to the uncompensated baseline, on the same order as the MMC system for similar idealized assumptions.

SUMMARY TABLE COMPARING MMC WITH NAV BASE FEEDBACK

MODEL	JITTER IN ARC SECONDS WINDOW SIZE (SECONDS)			
	1.0	9.0	60.0	1000.0
UNCOMPENSATED	.4698	1.005	1.945	2.498
MMC LAG = 10	.0399	.0603	.0658	.0659
NAV BASE FEEDBACK	.0556	.0939	.0981	.0981

BOTH MMC AND NAV BASE FEEDBACK SHOW SIGNIFICANT IMPROVEMENT OVER UNCOMPENSATED BASELINE JITTER AND STABILITY

SUMMARY

The salient points of the study are outlined on the summary chart below. As predicted in previous studies, the MMC technique is extremely effective at nulling jitter from rigid body motion. Excellent jitter compensation is theoretically possible for flexible modes as well. The study predicts jitter reduction factors of 5.4 for low frequency sources and 1.2 for high frequency sources. Stability reduction is even more dramatic, with factors as high as 17 predicted. However, it must be emphasized that extreme frequency sensitivity is characteristic of the MMC technique, limiting its use to linear systems which are empirically modeled to extreme fidelity. State of the art prediction techniques (finite element model normal modes analysis) for the modal parameters are insufficient to ensure acceptable performance.

The study also demonstrated the effectiveness of increased damping on jitter suppression, and its associated lessening of MMC frequency sensitivity with increased damping. It was also observed that errors in predicted damping had less adverse effects than similar errors in predicted frequency.

Multiple disturbances were explored and the MMC technique was seen to be effective here as well.

Finally, the MMC technique was compared to a primitive feedback system, and was seen to have similar limitations and effectiveness.

•RIGID BODY MOTION EFFECTIVELY NULLED

•FOR FLEXIBLE MODES:

LOW FREQUENCY RESPONSES CAN BE READILY SUPPRESSED

HIGH FREQUENCY RESPONSES MORE DIFFICULT TO CONTROL

HOWEVER:

ACCURATE DYNAMIC MODEL VITAL TO MMC EFFECTIVENESS FOR FLEXIBLE MODES

MMC HAS POTENTIAL APPLICATION FOR JITTER REDUCTION FOR NEXT GENERATION REMOTE SENSING SPACECRAFT

RECOMMENDATION

Due to the extreme frequency sensitivity displayed by the MMC technique, it is imperative that the system modal parameters be characterized with great accuracy. This necessitates the use of on-board measured data to characterize the dynamic behavior of the spacecraft. It is not possible to predict a priori the modal parameters to sufficient accuracy for the MMC technique to be effective.

USE ONBOARD MEASUREMENTS TO EXTRACT MODAL PARAMETERS

IMPLEMENT MMC USING MEASURED DATA TO SUPPRESS INSTRUMENT JITTER

USE GROUND DEMONSTRATION MODEL TO EVALUATE EFFECTIVENESS OF MMC TECHNIQUE

EXPERIMENTAL VALIDATION IS REQUIRED TO DEMONSTRATE FEASIBILITY OF MMC